

---

# A FEDERATED DISTRIBUTIONALLY ROBUST SUPPORT VECTOR MACHINE WITH MIXTURE OF WASSERSTEIN BALLS AMBIGUITY SET FOR DISTRIBUTED FAULT DIAGNOSIS

---

**Michael Ibrahim, Heraldo Rozas, Nagi Gebraeel, Weijun Xie**

H. Milton Stewart School of Industrial and Systems Engineering

Georgia Institute of Technology

Atlanta

{mibrahim41, heraldo.rozas, nagi, wxie}@gatech.edu

## ABSTRACT

The training of classification models for fault diagnosis tasks using geographically dispersed data is a crucial task for original parts manufacturers (OEMs) seeking to provide long-term service contracts (LTSCs) to their customers. Due to privacy and bandwidth constraints, such models must be trained in a federated fashion. Moreover, due to harsh industrial settings the data often suffers from feature and label uncertainty. Therefore, we study the problem of training a distributionally robust (DR) support vector machine (SVM) in a federated fashion over a network comprised of a central server and  $G$  clients without sharing data. We consider the setting where the local data of each client  $g$  is sampled from a unique true distribution  $\mathbb{P}_g$ , and the clients can only communicate with the central server. We propose a novel Mixture of Wasserstein Balls (MoWB) ambiguity set that relies on local Wasserstein balls centered at the empirical distribution of the data at each client. We study theoretical aspects of the proposed ambiguity set, deriving its out-of-sample performance guarantees and demonstrating that it naturally allows for the separability of the DR problem. Subsequently, we propose two distributed optimization algorithms for training the global FDR-SVM: i) a subgradient method-based algorithm, and ii) an alternating direction method of multipliers (ADMM)-based algorithm. We derive the optimization problems to be solved by each client and provide closed-form expressions for the computations performed by the central server during each iteration for both algorithms. Finally, we thoroughly examine the performance of the proposed algorithms in a series of numerical experiments utilizing both simulation data and popular real-world datasets.

## 1 Introduction

Original Equipment Manufacturers (OEMs) of capital-intensive assets such as gas turbines, aircraft engines, and mining equipment are increasingly implementing long-term service contracts (LTSCs) that can last for 10 to 20 years to ensure their products perform reliably over time [1]. Such contracts are beneficial to both the OEMs and the customers, as they provide the OEMs with a steady revenue stream, whereas they relieve the customers from all diagnosis and repair tasks in the occurrence of fault events. Indeed, one of the key services provided by the OEM as part of LTSCs is the diagnosis of any faults that may occur in the equipment used by the customers. Recently, many research efforts have been dedicated to performing fault diagnosis tasks by leveraging a wide array of data-driven Machine Learning (ML) classifiers. For example, ML models have been used in the fault diagnosis of motors [2], rotary machines [3], and pumps [4].

In the setting of an LTSC, the OEM's use of an ML model to perform fault diagnosis on the assets used by their customers presents a unique set of challenges. Firstly, the ML model would need to be trained on geographically-dispersed historical operation data obtained from all the customers' sites. However, the sharing of large volumes of high-dimensional data collected by today's advanced sensors from the customers to the OEM can be infeasible due to bandwidth restrictions and data transfer costs. Additionally, customers are increasingly incorporating privacy and ownership stipulations in their LTSCs, which limits the OEM's access to sensitive operational data and prevents data sharing. Secondly, the harsh industrial environments contribute significant noise to the data, making analysis

even more difficult. This problem is further compounded by the inconsistent accuracy in the labeling of fault events stemming from the wide variability in operator skill levels and expertise.

The recently developed field of Federated Learning (FL) [5] offers a natural solution for OEMs to train fault classification models without requiring the customers to share their local operation data. Indeed, FL has been utilized successfully in [6] to develop a distributed framework for machinery fault diagnosis. However, while FL addresses the distributed nature of the training data, it does not necessarily provide rigorous methods for modeling the uncertainty in the data or errors in event labels.

To model the feature and label noise in a binary classification problem, one can view the data features  $\mathbf{x} \in \mathcal{X} \subseteq \mathbb{R}^P$  and labels  $y \in \{-1, +1\}$  as random variables governed by some underlying distribution  $\mathbb{P}$  [7]. Therefore, a classifier characterized by loss function  $\ell(\mathbf{w}; (\mathbf{x}, y))$  parameterized by  $\mathbf{w} \in \mathbb{R}^P$  would ideally be trained by minimizing the expected risk  $\mathbb{E}^{\mathbb{P}}[\ell(\mathbf{w}; (\mathbf{x}, y))]$ . In practice, however, the expected risk minimization problem is often impossible to solve due to  $\mathbb{P}$  being unknown. This issue is traditionally addressed via the sample average approximation (SAA) [8], whereby a training dataset comprised of  $N$  independent and identically distributed (IID) samples  $\{(\hat{\mathbf{x}}, \hat{y})_n\}_{n=1}^N$  is used to approximate  $\mathbb{P}$  via a distribution  $\hat{\mathbb{P}}_N$ . Usually  $\hat{\mathbb{P}}_N$  is the empirical distribution of the training data for classification models. Subsequently, the model is trained by minimizing the empirical risk  $\mathbb{E}^{\hat{\mathbb{P}}_N}[\ell(\mathbf{w}; (\mathbf{x}, y))]$ . However, in cases where the training data is noisy or limited the resulting model can be highly suboptimal, leading to poor out-of-sample performance [7, 9, 10].

The recently popularized field of distributionally robust optimization (DRO) [9–15] offers a solution to the challenge of data uncertainty. More specifically, it hedges against the uncertainty in the data by first defining a set of distributions referred to as the ambiguity set  $\mathcal{A}$ . Subsequently, the model is trained by minimizing the worst-case risk  $\sup_{\mathbb{Q} \in \mathcal{A}} \mathbb{E}^{\mathbb{Q}}[\ell(\mathbf{w}; (\mathbf{x}, y))]$  attained by any distribution  $\mathbb{Q} \in \mathcal{A}$ . This is because minimizing the worst-case risk indirectly reduces the expected risk if  $\mathbb{P} \in \mathcal{A}$  [9]. Many works in the literature explore various methods of defining the ambiguity set  $\mathcal{A}$ . For example, works such as [11, 12] define  $\mathcal{A}$  as a set of all distributions that obey certain moment constraints. Alternatively, works such as [13, 16] and [9, 10, 17] define  $\mathcal{A}$  as a set of all distributions that are a distance  $\varepsilon$  away from a nominal distribution  $\mathbb{P}_0$  in the sense of  $\phi$ -divergences and the Wasserstein distance, respectively. However, much of the existing literature on Wasserstein DRO implicitly assumes that the training data is stored centrally on a single server [7, 10, 15, 17]. Extending DR ML models to federated settings where data cannot be shared is not trivial [18].

Numerous research efforts have successfully improved the performance of traditional classifiers by using DRO. This includes logistic regression [7], support vector machines (SVM) [15, 19], and deep neural networks (DNNs) [20]. Similarly, many research efforts have also proposed the training of various classifiers in a federated fashion, such as DNNs [6], kernel SVMs [21], and  $k$  nearest neighbors (kNN) [22]. However, to the best of our knowledge, there is currently no work that develops a distributionally robust classifier that hedges against feature and label uncertainty simultaneously and can be trained in a federated fashion without sharing data.

In this paper, we develop a federated distributionally robust support vector machine (FDR-SVM) that can be trained collaboratively by a central server (the OEM)  $G$  clients (the customers). To this end, we introduce a novel Mixture of Wasserstein Balls (MoWB) ambiguity set, which relies on local Wasserstein balls centered at the empirical distribution  $\hat{\mathbb{P}}_{N_g}$  of the data at each client  $g$ , for  $g \in G$ . We examine the out-of-sample performance of the MoWB ambiguity set, and demonstrate that it naturally leads to the separability of the FDR-SVM problem. Subsequently, we derive and implement two distributed optimization algorithms for training the proposed FDR-SVM. The contributions of our paper can be summarized as follows:

- i. We propose the MoWB ambiguity set, which extends the conventional Wasserstein ball to the distributed setting. Our proposed ambiguity set contains mixtures of distributions from Wasserstein balls defined locally at each client. Using this ambiguity set, we reformulate the FDR-SVM problem into a separable form that can be solved in a distributed manner without sharing data. We also derive out-of-sample performance guarantees for the MoWB ambiguity set under certain assumptions.
- ii. We propose two different distributed algorithms to train our proposed FDR-SVM: a subgradient method-based algorithm (SM algorithm), and an alternating direction method of multipliers-based algorithm (ADMM algorithm). We propose two distributed algorithms for training the FDR-SVM: a subgradient method-based algorithm (SM algorithm) and an alternating direction method of multipliers-based algorithm (ADMM algorithm). In both approaches, we outline the specific optimization problems solved by each client and the update rules the central server uses to update its global model in each iteration.
- iii. We conduct a theoretical analysis of our proposed algorithms, covering both convergence and time complexity. Specifically, we show that the SM algorithm converges with an appropriately chosen step size, while the ADMM

algorithm requires an additional regularization term to ensure theoretical convergence. We also derive the time complexity for both algorithms, expressed in terms of the number of clients, training samples, and features.

- iv. We perform various experiments using simulation and popular real-world datasets, in which we thoroughly examine the performance of our FDR-SVM and the two algorithms used to train it.

The rest of this paper is organized as follows. Section 2 provides a summary of the works relevant to the FDR-SVM, covering topics of DRO, FL, and their combination. Section 3 provides a brief background on the theoretical aspects of Wasserstein DRO, as well as a summary of the problem setup. Section 4 introduces the proposed MoWB ambiguity set and demonstrates how the MoWB ambiguity set leads to problem separability. Section 5 describes the algorithms proposed to train the FDR-SVM and discusses their theoretical guarantees. Section 6 contains our numerical experiments, and finally Section 7 provides some concluding remarks.

## 2 Related Works

### 2.1 Distributionally Robust Classifiers

Many existing works in the literature seek to develop DR versions of common classifiers to improve their out-of-sample performance. For example, the authors in [7] and [15] develop Wasserstein DR versions of logistic regression and hard and soft-margin SVMs, respectively. They provide tractable, convex reformulations for their proposed DR problems, leveraging popular duality results from [9, 10]. This work is extended in [23], where the authors derive a tractable, convex reformulation of a Wasserstein DR logistic regression model for data with mixed features, demonstrating that considering categorical data leads to a fundamentally different problem.

Alternatively, the authors in [24] utilize a moment-based ambiguity set to derive a DR SVM. They do so by writing the ambiguity set as a projection of a larger set and leveraging duality results to rewrite infinite dimensional problems in the constraints as finite-dimensional ones under additional constraints. Similarly, the authors in [19] develop a DR chance-constrained kernel SVM using a moment-based ambiguity set. They derive a tractable second-order cone programming (SOCP) reformulation of their problem utilizing empirical moment information, and they propose an ADMM-based algorithm to train their model.

Finally, the authors in [20] utilize group DRO to address the tendency of classification deep neural networks (DNNs) to learn spurious correlations in the data. More specifically, they manually group the training data according to those correlations and minimize the risk with respect to the worst-case group. However, the key challenge in that work is that data grouping has to be performed manually, which can be extremely difficult for very large datasets. This challenge is addressed by the authors in [25], where they utilize a DNN to perform the data grouping. The common aspect shared between the previously listed works is that they rely on the training data being present at a central location. Indeed as argued in [18], this can make such models difficult to extend to distributed settings.

### 2.2 Federated Learning and Distributed Model Training

Federated learning (FL) was first introduced in the quintessential work presented in [5], where the authors develop a framework for training DNNs in a distributed, privacy-preserving fashion. Their proposed federated averaging (FedAvg) algorithm relies on the iterative averaging of locally trained models. The authors demonstrate that their model performs well even in settings with highly imbalanced, non-IID data. This is further developed in [26], where the authors propose a sparse ternary compression technique (STC) to reduce local model complexity, thereby reducing communication costs. However, the authors in [27] argue that since STC performs compression after the training is complete, the quantization is not optimized during training. Instead, they propose the use of ternary quantization in the local model training to simplify the models, thereby further reducing communication costs. Other works in the literature aim to improve FL in settings where client data is highly heterogeneous, a summary of which is provided in the survey presented in [28]. One such work is [29], where the authors utilize concepts from multi-task learning (MTL) to introduce clustered federated learning (CFL). Their framework allows each client to train a version of the global model that is specialized for their local data.

Various works in the literature leverage concepts from FL to train statistical ML models in a distributed fashion. For example, the authors in [21] develop a kernel SVM that can be trained in a federated manner while achieving low memory consumption and fast convergence for the local model training by using a block boosting algorithm. Similarly, the authors in [30] develop a federated kernel k-means model that is both memory and communication efficient. To directly address the data heterogeneity across clients, the authors in [31] combine concepts from MTL and FL to train an SVM in a distributed fashion. They utilize an ADMM algorithm for their model training, whereby each client trains a version of the global model parameters that is specialized for their unique local data. Similarly, the authors in [32]

develop an accelerated ADMM algorithm for the parallel distributed training of an  $\ell_2$ -norm regularized SVM. Finally, the authors in [22] develop a secure and efficient distributed k-nearest-neighbors (kNN) classifier that relies on data encryption to preserve privacy.

A different approach to training an SVM in a distributed manner is presented in [33]. In this work, the authors propose the distributed training of a global SVM model over a strongly connected network to leverage parallel computing in the training process. However, it must be noted that the authors of this work are motivated by exploiting parallel computing in the training rather than preserving privacy or avoiding the costs of data sharing. Thus, a minimal amount of data samples may be shared between clients in this framework.

### 2.3 Distributionally Robust Federated Learning

Various works in the literature combine concepts from DRO and FL. For example, the authors in [34] develop a DR version of FedAvg where the clients can only communicate with the central server. Distributional robustness in this setting hedges against the uncertainty in the client weights. The authors propose a communication-efficient algorithm to solve the DR problem and study its convergence. This is extended in [35], where the authors propose a generalized framework to address issues of data heterogeneity across clients and high levels of noise in the data. They address the latter issue by utilizing mixup techniques in the local training stages of the federated framework. In contrast, the authors in [36] develop a communication efficient algorithm for the DR FedAvg problem in the fully decentralized setting without a central server.

Another research direction that combines elements of DRO and FL is explored in [37] where the authors develop a Wasserstein ambiguity set using barycenters. In this setting, the authors consider multiple clients, each of which has local samples from  $\mathbb{P}$  allowing it to construct a local empirical distribution  $\widehat{\mathbb{P}}_{N_g}$ . The global ambiguity set is then centered around the barycenter (which is similar to a mean) of all  $\{\widehat{\mathbb{P}}_{N_g}\}_{g=1}^G$ . However, the barycenter is not always guaranteed to exist and can be difficult to compute in a distributed fashion when it does. Similarly, the authors in [18] study a multi-client network where each client has access to a finite number of samples from  $\mathbb{P}$ . The clients seek to collaborate via P2P communication to solve a Wasserstein DRO problem in a distributed fashion. The authors show that the reformulation of the Wasserstein DRO problem in [9, 10] admits a reformulation that can be solved in a distributed fashion via Lagrange duality if the clients can communicate with each other.

## 3 Preliminaries

### 3.1 Distributionally Robust Optimization

The DRO problem is mathematically formulated as follows [38]:

$$\inf_{\ell \in \mathcal{L}} \sup_{\mathbb{Q} \in \mathcal{A}} \mathbb{E}^{\mathbb{Q}}[\ell], \quad (1)$$

where  $\ell$  is the loss function belonging to a set  $\mathcal{L}$  of all loss functions under study, and  $\mathbb{Q}$  is any distribution within ambiguity set  $\mathcal{A}$ .

As discussed in many works such as [9, 10, 13, 14, 17], problem (1) admits convex, tractable reformulations in many cases of practical interest. In this work, we focus on DRO utilizing ambiguity sets defined via the Wasserstein distance [39] due to its attractive properties [9, 17]. These properties include the set's capacity to encompass both continuous and discrete distributions regardless of the structure of the nominal distribution  $\mathbb{P}_0$ . Additionally, one can derive guarantees that  $\mathbb{P} \in \mathcal{A}$  with a given confidence level, provided certain mild assumptions are satisfied. We utilize the empirical distribution of the data  $\widehat{\mathbb{P}}_N$  as the nominal distribution  $\mathbb{P}_0$ , and express the Wasserstein ambiguity set (Wasserstein ball)  $\mathcal{A}_{\varepsilon, q, d}(\Xi)$  as,

$$\mathcal{A}_{\varepsilon, q, d}(\Xi) := \left\{ \mathbb{Q} \in \mathcal{P}(\Xi) : W_{d, q}(\mathbb{Q}, \widehat{\mathbb{P}}_N) \leq \varepsilon \right\}, \quad (2)$$

where  $\mathcal{P}(\Xi)$  is the set of all distributions supported on  $\Xi$ , and  $W_{d, q}(\cdot, \cdot)$  is the type- $q$  Wasserstein distance equipped with transportation cost function  $d(\xi, \xi')$ . In our work we utilize the type-1 Wasserstein distance and the separable cost function introduced in [7, 15], defined as follows:

$$d(\xi, \xi') := \|\mathbf{x} - \mathbf{x}'\| + \kappa \mathbb{1}_{\{y \neq y'\}}, \quad (3)$$

where  $\|\cdot\|$  is any common norm on  $\mathbb{R}^P$ , and  $\kappa$  is a parameter corresponding to label flipping cost.

### 3.2 Problem Setup

We consider the problem of classifying data of the form  $\xi = (\mathbf{x}, y)$  distributed over  $G$  clients, where  $\mathbf{x} \in \mathcal{X} \subseteq \mathbb{R}^P$  is the feature vector and  $y \in \{-1, 1\}$  is the label. We consider classification via the binary support vector machine (SVM) characterized by the hinge loss function  $\ell_H(\mathbf{w}; \xi)$  parameterized by  $\mathbf{w} \in \mathbb{R}^P$  and defined as  $\ell_H(\mathbf{w}; \xi) = \max\{0, 1 - y \cdot \mathbf{w}^\top \mathbf{x}\}$ . We choose the SVM classifier as it is a well-established model that is commonly used in fault classification settings [4, 40]. Moreover, our consideration of a binary classifier does not lead to loss of generality. This is because binary classifiers are commonly directly extended in practice to multiclass problems via a one-vs-all or a one-vs-one framework.

We study a federated learning setting where clients can only communicate with the central server but not with each other. Clients do not share their data with the central server, but they can transmit insights from locally trained models such as local (sub)gradients or model parameters. In this context, we assume the existence of a training set  $\mathcal{S} = \{\widehat{\xi}_n\}_{n=1}^N = \{(\widehat{\mathbf{x}}_n, \widehat{y}_n)\}_{n=1}^N$ , which is divided into  $G$  groups with each group  $g \in [G]$  containing  $N_g$  training samples. We denote the empirical distribution of the  $N_g$  training samples at the  $g^{\text{th}}$  client as  $\widehat{\mathbb{P}}_{N_g}$  and the true distribution governing its data as  $\mathbb{P}_g$ .

## 4 MoWB Ambiguity Set and Its Properties

### 4.1 Problem Separability

In this section, we extend the traditional Wasserstein ball to the distributed setting via the novel MoWB ambiguity set  $\mathcal{A}_G$  defined next.

**Definition 1** (MoWB ambiguity set). The Mixture of Wasserstein Balls (MoWB) ambiguity set contains mixture distributions whose constituents are distributions from local Wasserstein balls defined at each client, and is defined as

$$\mathcal{A}_G := \left\{ \mathbb{Q}: \mathbb{Q} = \sum_{g=1}^G \alpha_g \mathbb{Q}_g, \alpha_g \geq 0, \sum_{g=1}^G \alpha_g = 1, \mathbb{Q}_g \in \mathcal{A}_{\varepsilon_g, 1, d}^{(g)}(\Xi) \right\}, \quad (4)$$

where  $\alpha_g$  is the fixed weight of each client  $g$ , and  $\mathcal{A}_{\varepsilon_g, 1, d}^{(g)}(\Xi)$  is the type-1 Wasserstein ball of radius  $\varepsilon_g$  supported on  $\Xi$ , centered at  $\widehat{\mathbb{P}}_{N_g}$ , and defined via transportation cost function  $d$  in expression (3).

*Remark 1.* Observe that when  $G = 1$ , our proposed ambiguity set reduces to the conventional Wasserstein ball  $\mathcal{A}_{\varepsilon, q, d}(\Xi)$  defined in (2). This suggests that our proposed ambiguity set indeed naturally extends the conventional Wasserstein ball to the distributed setting, allowing for the problem to be reformulated in a separable fashion as we demonstrate next.

**Lemma 1** (Problem Separability). *The original DRO problem in (1) equipped with the MoWB ambiguity set defined in (4) admits the following reformulation:*

$$\inf_{\mathbf{w}} \sup_{\mathbb{Q} \in \mathcal{A}_G} \mathbb{E}^{\mathbb{Q}}[\ell_H(\mathbf{w}; \xi)] = \inf_{\mathbf{w}} \sum_{g=1}^G \alpha_g \sup_{\mathbb{Q}_g \in \mathcal{A}_{\varepsilon_g, 1, d}^{(g)}(\Xi)} \mathbb{E}^{\mathbb{Q}_g}[\ell_H(\mathbf{w}; \xi)]. \quad (5)$$

*Proof.*

$$\inf_{\mathbf{w}} \sup_{\mathbb{Q} \in \mathcal{A}_G} \mathbb{E}^{\mathbb{Q}}[\ell_H(\mathbf{w}; \xi)] \quad (6a)$$

$$= \inf_{\mathbf{w}} \sup_{\{\mathbb{Q}_g \in \mathcal{A}_{\varepsilon_g, 1, d}^{(g)}(\Xi)\}_{g=1}^G} \mathbb{E}^{\sum_{g=1}^G \alpha_g \mathbb{Q}_g}[\ell_H(\mathbf{w}; \xi)] \quad (6b)$$

$$= \inf_{\mathbf{w}} \sup_{\{\mathbb{Q}_g \in \mathcal{A}_{\varepsilon_g, 1, d}^{(g)}(\Xi)\}_{g=1}^G} \sum_{g=1}^G \alpha_g \mathbb{E}^{\mathbb{Q}_g}[\ell_H(\mathbf{w}; \xi)] \quad (6c)$$

$$= \inf_{\mathbf{w}} \sum_{g=1}^G \alpha_g \sup_{\mathbb{Q}_g \in \mathcal{A}_{\varepsilon_g, 1, d}^{(g)}(\Xi)} \mathbb{E}^{\mathbb{Q}_g}[\ell_H(\mathbf{w}; \xi)], \quad (6d)$$

where (6b) follows from the definition of the global ambiguity  $\mathcal{A}_G$  set in (4), (6c) follows from the law of expectation over mixture distributions, and (6d) follows by recognizing that the maximization problems are separable due to each decision variable only affecting its corresponding term.  $\square$

We observe that the reformulation in (5) can be efficiently solved in a distributed fashion. Each client only needs to solve their own inner maximization problem and then send the results to the central server. The server uses this information to solve the outer minimization problem. Next, we briefly study the out-of-sample performance of our MoWB ambiguity set and then discuss our two proposed solutions algorithms in Section 5.

## 4.2 Out-of-Sample Performance Guarantees

Since the MoWB ambiguity set  $\mathcal{A}_G$  relies on local Wasserstein balls  $\mathcal{A}_{\varepsilon_g, 1, d}^{(g)}(\Xi)$ , it inherits desirable out-of-sample performance guarantees discussed in [7, 9]. To see this, first observe that by construction of our problem the true distribution  $\mathbb{P}$  governing the data at all clients can be written as  $\mathbb{P} = \sum_{g=1}^G \alpha_g \mathbb{P}_g$  where  $\mathbb{P}_g$  is the distribution governing the local data at client  $g$ . In practice, the client weights  $\alpha_g$  would be set by the central server prior to model training in one of various ways. For example, they could be equal for all clients, or treated as tuning parameters. We combine this fact with the following assumptions to reach our out-of-sample performance result.

**Assumption 1** (Independence of Training Data). All the training samples  $\{(\widehat{\mathbf{x}}_{(n_g)}, \widehat{\mathbf{y}}_{(n_g)})\}_{n=1}^N$  at client  $g$  are IID samples from its true distribution  $\mathbb{P}_g$ .

**Assumption 2** (Light-tailed Distribution [7]). The true distribution  $\mathbb{P}_g$  of the data at client  $g$  is light-tailed. That is, there exists  $a > 1$  with  $A_g := \mathbb{E}^{\mathbb{P}_g}[\exp(\|2\mathbf{x}\|^{a_g})] < +\infty$ .

**Proposition 1** (Out-of-Sample Performance). *Suppose Assumptions 1 and 2 hold and the local Wasserstein ball radius  $\varepsilon_g$  at client  $g$  is set as described in Theorem 18 of [9], shown next*

$$\varepsilon_{N_g}(\eta_g) = \left( \frac{\log(c_{1_g} \eta_g^{-1})}{c_{2_g} N_g} \right)^{\frac{1}{a_g}} \mathbb{1}_{\left\{ N_g < \frac{\log(c_{1_g} \eta_g^{-1})}{c_{2_g} c_{3_g}} \right\}} + \left( \frac{\log(c_{1_g} \eta_g^{-1})}{c_{2_g} N_g} \right)^{\frac{1}{P}} \mathbb{1}_{\left\{ N_g \geq \frac{\log(c_{1_g} \eta_g^{-1})}{c_{2_g} c_{3_g}} \right\}},$$

where  $c_{1_g}, c_{2_g}, c_{3_g} \in \mathbb{R}_+$  depend only on the parameters  $a_g$  and  $A_g$ , the dimension  $P$  of the feature space, and the transportation cost in (3). Then the MoWB ambiguity set  $\mathcal{A}_G$  defined in (4) enjoys the following property

$$\mathbb{P}^N \{ \mathbb{P} \in \mathcal{A}_G \} \geq \prod_{g=1}^G (1 - \eta_g),$$

where each  $\eta_g$  is such that  $\mathbb{P}^{N_g} \{ \mathbb{P}_g \in \mathcal{A}_{\varepsilon_g, 1, d}^{(g)}(\Xi) \} \geq (1 - \eta_g)$ .

*Proof.* Suppose the assumptions in the Proposition statement hold. Then we have the following

$$\mathbb{P}^{N_g} \{ \mathbb{P}_g \in \mathcal{A}_{\varepsilon_g, 1, d}^{(g)}(\Xi) \} \geq (1 - \eta_g)$$

Therefore, we can obtain the following

$$\mathbb{P}^N \{ \mathbb{P} \in \mathcal{A}_G \} \geq \prod_{g=1}^G \mathbb{P}^{N_g} \{ \mathbb{P}_g \in \mathcal{A}_{\varepsilon_g, 1, d}^{(g)}(\Xi) \} \tag{7a}$$

$$\geq \prod_{g=1}^G (1 - \eta_g), \tag{7b}$$

where (7a) follows by noting that the local data and Wasserstein balls at all  $G$  clients are mutually independent, and that  $\mathbb{P} = \sum_{g=1}^G \alpha_g \mathbb{P}_g$ . Furthermore, note that (7a) contains an inequality instead of an equality as there is no guarantee that  $\mathbb{P}$  cannot be constructed as a mixture of distributions from the local Wasserstein balls  $\{ \mathcal{A}_{\varepsilon_g, 1, d}^{(g)}(\Xi) \}_{g=1}^G$ . Therefore, we have that

$$\mathbb{P}^N \left\{ \mathbb{P} \in \mathcal{A}_G \cap \mathbb{P}_g \notin \{ \mathcal{A}_{\varepsilon_g, 1, d}^{(g)}(\Xi) \}_{g=1}^G \right\} \neq 0.$$

□

*Remark 2.* Beyond its desirable out-of-sample performance properties, our proposed MoWB ambiguity set also inherits other desirable properties from the traditional Wasserstein ambiguity set listed in [9]. One key property is the ability of the MoWB ambiguity set to anticipate black swans by possibly assigning probability mass to any point in the support set  $\Xi$  regardless of the structure of  $\widehat{\mathbb{P}}_{N_g}$  for all  $g \in [G]$ .

## 5 Solution Algorithms

In this section, we present two algorithms for solving the reformulated problem expressed in (5), in a distributed manner. The first algorithm is a subgradient method-based algorithm (SM algorithm) and the second is an ADMM algorithm. We begin by making the following assumption.

**Assumption 3** (Synchronous Training). The distributed optimization problem in (5) is solved synchronously. That is, the central server only performs an update step once all the clients have completed solving their local problems and communicated their insights to the central server.

### 5.1 SM Algorithm

The SM algorithm begins by initializing the global model parameters  $\mathbf{w}$ . Next, each client  $g$  seeks to obtain a subgradient for their respective inner maximization problem from the reformulated problem in (5). This requires each client  $g$  to obtain a worst-case distribution  $\mathbb{Q}_g^*$  from its local ambiguity set  $\mathcal{A}_{\varepsilon_g, 1, d}^{(g)}(\Xi)$ , allowing the worst-case risk to be directly expressed as an expectation with respect to  $\mathbb{Q}_g^*$ . However, as is discussed in [9, 10], the worst-case distribution cannot be obtained from a type-1 Wasserstein ambiguity set centered around an empirical distribution  $\widehat{\mathbb{P}}_{N_g}$  if  $\mathcal{X}$  is not compact. Therefore, we make the following assumption for the SM algorithm.

**Assumption 4** (Support of Feature Vector). The feature vector  $\mathbf{x}$  is such that:  $0 \leq e_p^\top \mathbf{x} \leq 1 \forall p \in [P]$ , where  $e_p$  are the standard unit vectors.

*Remark 3.* We note that Assumption 4 is not very restrictive in many practical cases. This is because real-world data is often bounded by the ranges of the sensor measurements used for data acquisition. Therefore, it can be easily normalized using those ranges. It should be noted, however, that in some settings, normalizing the data can lead to of important features. In such cases, one may instead choose to modify the worst-case distribution problem using information about the support of the feature, as shown in (8).

In other words, if Assumption 4 is satisfied and the global model parameters  $\mathbf{w}$  are fixed, then it can be shown that the worst-case distribution  $\mathbb{Q}_g^*$  for client  $g$  can be written as follows [15]:

$$\mathbb{Q}_g^* = \frac{1}{N_g} \sum_{n_g=1}^{N_g} \left( \beta_{n_g}^+ \delta_{(\widehat{\mathbf{x}}_{n_g} - \mathbf{q}_{n_g}^+ / \beta_{n_g}^+, \widehat{y}_{n_g})} + \beta_{n_g}^- \delta_{(\widehat{\mathbf{x}}_{n_g} - \mathbf{q}_{n_g}^- / \beta_{n_g}^-, -\widehat{y}_{n_g})} \right), \quad (8)$$

where  $\delta_{(\mathbf{x}, y)}$  is the Dirac density function assigning probability mass 1 at sample  $\boldsymbol{\xi} = (\mathbf{x}, y)$ , and  $\beta_{n_g}^+, \beta_{n_g}^-, \mathbf{q}_{n_g}^+$ , and  $\mathbf{q}_{n_g}^-$  are the maximizers to the following problem:

$$\max_{\substack{\beta_{n_g}^+, \beta_{n_g}^- \\ \mathbf{q}_{n_g}^+, \mathbf{q}_{n_g}^-}} H_g(\mathbf{w}) = \begin{cases} \max_{\substack{\beta_{n_g}^+, \beta_{n_g}^- \\ \mathbf{q}_{n_g}^+, \mathbf{q}_{n_g}^-}} \frac{1}{N_g} \sum_{n_g=1}^{N_g} \left( -(\beta_{n_g}^+ - \beta_{n_g}^-) \widehat{y}_{n_g} \mathbf{w}^\top \widehat{\mathbf{x}}_{n_g} - \widehat{y}_{n_g} \mathbf{w}^\top (\mathbf{q}_{n_g}^+ - \mathbf{q}_{n_g}^-) \right) \\ \text{s. t.} & \sum_{n_g=1}^{N_g} (\|\mathbf{q}_{n_g}^+\| + \|\mathbf{q}_{n_g}^-\| + \kappa_g \beta_{n_g}^-) \leq N_g \varepsilon_g \\ & \beta_{n_g}^+ + \beta_{n_g}^- = 1 & \forall n_g \in [N_g] \\ & 0 \leq \beta_{n_g}^+ \widehat{\mathbf{x}}_{n_g} - \mathbf{q}_{n_g}^+ \leq \beta_{n_g}^+ & \forall n_g \in [N_g] \\ & 0 \leq \beta_{n_g}^- \widehat{\mathbf{x}}_{n_g} - \mathbf{q}_{n_g}^- \leq \beta_{n_g}^- & \forall n_g \in [N_g] \\ & \beta_{n_g}^+, \beta_{n_g}^- \geq 0 & \forall n_g \in [N_g] \end{cases}, \quad (9)$$

where  $\|\cdot\|$  is the norm used in the definition of the transportation cost function (3).

Armed with the discrete worst-case distribution  $\mathbb{Q}_g^*$ , each client  $g$  can now obtain a subgradient to its respective inner maximization problem, simply by obtaining a subgradient of  $\mathbb{E}^{\mathbb{Q}_g^*}[\ell_H(\mathbf{w}; \boldsymbol{\xi})]$ . This is because, by definition,  $\mathbb{Q}_g^*$  attains the worst-case risk. Therefore, a subgradient for the local risk maximization problem can be obtained from the

following

$$\partial \sup_{\mathbb{Q}_g \in \mathcal{A}_{\varepsilon_g, 1, d}^{(g)}(\Xi)} \mathbb{E}^{\mathbb{Q}_g}[\ell_H(\mathbf{w}; \boldsymbol{\xi})] \supseteq \partial \mathbb{E}^{\mathbb{Q}_g^*}[\ell_H(\mathbf{w}; \boldsymbol{\xi})] \quad (10a)$$

$$= \mathbb{E}^{\mathbb{Q}_g^*}[\partial \ell_H(\mathbf{w}; \boldsymbol{\xi})] \quad (10b)$$

$$= \frac{1}{N_g} \sum_{n_g=1}^{N_g} (\mathcal{A}^+ + \mathcal{A}^-), \quad (10c)$$

where (10a) follows from Lemma 4.4.1 in [41], (10b) follows from the fact that  $\ell(\boldsymbol{\xi})$  is convex and integrable, and (10c) follows from the fact that  $\mathbb{P}_g^*$  is a discrete distribution, thus  $\mathbb{E}^{\mathbb{Q}_g^*}[\cdot]$  is a weighted sum. In the above,  $+$  denotes the Minkowski sum and the sets  $\mathcal{A}^+$  and  $\mathcal{A}^-$  are defined as follows:

$$\mathcal{A}^\pm = \begin{cases} \mathbf{0} & \text{if } 1 \mp \widehat{\mathbf{y}}_{n_g} \cdot \mathbf{w}^\top \widehat{\mathbf{z}}_{n_g}^\pm < 0 \\ \mp \beta_{n_g}^\pm \widehat{\mathbf{y}}_{n_g} \widehat{\mathbf{z}}_{n_g}^\pm & \text{if } 1 \mp \widehat{\mathbf{y}}_{n_g} \cdot \mathbf{w}^\top \widehat{\mathbf{z}}_{n_g}^\pm > 0, \\ \text{conv}(\{\mathbf{0}, \mp \beta_{n_g}^\pm \widehat{\mathbf{y}}_{n_g} \widehat{\mathbf{z}}_{n_g}^\pm\}) & \text{if } 1 \mp \widehat{\mathbf{y}}_{n_g} \cdot \mathbf{w}^\top \widehat{\mathbf{z}}_{n_g}^\pm = 0 \end{cases}$$

where  $\widehat{\mathbf{z}}_{n_g}^\pm = \widehat{\mathbf{x}}_{n_g} - \mathbf{q}_{n_g}^{\pm*} / \beta_{n_g}^{\pm*}$ , and  $\text{conv}(\Theta)$  is the convex hull of set  $\Theta$ .

The computed local subgradients are sent to the central server, which computes a weighted sum of the subgradients using weights  $\alpha_g$ , and performs a subgradient step on the model parameters  $\mathbf{w}$ . The central server then sends the updated  $\mathbf{w}$  to the clients and the process repeats until convergence, which we discuss in further detail later. We write our SM algorithm explicitly as follows:

---

#### Algorithm 1 SM Algorithm

---

**Input:**  $\mathbf{w}^{(0)}$

**Parameters:** Number of iterations  $T$ , stepsize  $\gamma(t)$  at iteration  $t$

**Output:**  $\mathbf{w}^*$

- 1: **for**  $t = 1, \dots, T$  **do**
  - 2:   **for** clients  $g = 1, \dots, G$  **do**
  - 3:      $[\beta_{n_g}^{+*}, \beta_{n_g}^{-*}, \mathbf{q}_{n_g}^{+*}, \mathbf{q}_{n_g}^{-*}] \leftarrow \arg \max_{\beta_{n_g}^+, \beta_{n_g}^-, \mathbf{q}_{n_g}^+, \mathbf{q}_{n_g}^-} H_g(\mathbf{w}^{(t)})$
  - 4:      $\mathbb{Q}_g^* \leftarrow \frac{1}{N_g} \sum_{n_g=1}^{N_g} \beta_{n_g}^{+*} \delta_{(\widehat{\mathbf{x}}_{n_g} - \mathbf{q}_{n_g}^{+*} / \beta_{n_g}^{+*}, \widehat{\mathbf{y}}_{n_g})} + \beta_{n_g}^{-*} \delta_{(\widehat{\mathbf{x}}_{n_g} - \mathbf{q}_{n_g}^{-*} / \beta_{n_g}^{-*}, -\widehat{\mathbf{y}}_{n_g})}$
  - 5:      $\mathbf{v}_g \leftarrow$  any  $\mathbf{u}$  such that  $\mathbf{u} \in \partial \mathbb{E}^{\mathbb{Q}_g^*}[\ell_H(\mathbf{w}; \boldsymbol{\xi})]$
  - 6:   **end for**
  - 7:    $\mathbf{w}^{(t+1)} \leftarrow \mathbf{w}^{(t)} - \gamma(t) \sum_{g=1}^G \alpha_g \mathbf{v}_g$
  - 8: **end for**
- 

## 5.2 ADMM Algorithm

The ADMM algorithm requires each client  $g$  to solve their own local problem and shares their optimal local model  $\mathbf{w}_g^*$  with the central server. The central server then proceeds to aggregate the local models to obtain an optimal global model  $\mathbf{w}^*$ , which it sends to the clients. The process repeats until convergence, which we discuss in further detail later.

To derive this algorithm theoretically, we begin by introducing a decision variable  $\mathbf{w}_g$  for each client  $g$ , and rewriting the problem in (5) as follows:

$$\begin{aligned} \inf_{\mathbf{w}_g, \mathbf{w}} \quad & \sum_{g=1}^G \alpha_g \sup_{\mathbb{Q}_g \in \mathcal{A}_{\varepsilon_g, 1, d}^{(g)}(\Xi)} \mathbb{E}^{\mathbb{Q}_g}[\ell_H(\mathbf{w}_g; \boldsymbol{\xi})] \\ \text{s. t.} \quad & \mathbf{w}_g - \mathbf{w} = 0 \quad \forall g \in [G]. \end{aligned} \quad (11)$$

We express the Augmented Lagrangian parameterized by  $\rho$  for the problem in (5) as follows:

$$\mathcal{L}_\rho(\lambda_1, \dots, \lambda_G, \mathbf{w}_1, \dots, \mathbf{w}_G, \mathbf{w}, \boldsymbol{\mu}_1, \dots, \boldsymbol{\mu}_G) = \sum_{g=1}^G \alpha_g \mathcal{L}_{\rho, g}(\lambda_g, \mathbf{w}_g, \mathbf{w}, \boldsymbol{\mu}_g),$$

where  $\boldsymbol{\mu}_g$  is the scaled Lagrange multiplier for the  $g^{\text{th}}$  client, and

$$\mathcal{L}_{\rho,g}(\lambda_g, \mathbf{w}_g, \mathbf{w}, \boldsymbol{\mu}_g) = \sup_{\mathbb{Q}_g \in \mathcal{A}_{\varepsilon_g, 1, d}^{(g)}(\Xi)} \mathbb{E}^{\mathbb{Q}_g}[\ell_H(\mathbf{w}_g; \boldsymbol{\xi})] + \frac{\rho}{2} \|\mathbf{w}_g - \mathbf{w} + \boldsymbol{\mu}_g\|_2^2.$$

Now observe that the objective function in (11) does not contain any terms with  $\mathbf{w}$ . Therefore, each client needs only minimize their own Augmented Lagrangian  $\mathcal{L}_{\rho,g}(\lambda_g, \mathbf{w}_g, \mathbf{w}, \boldsymbol{\mu}_g)$  with respect to  $\mathbf{w}_g$  as follows:

$$J_g(\mathbf{w}, \boldsymbol{\mu}_g) = \inf_{\mathbf{w}_g} \mathcal{L}_{\rho,g}(\lambda_g, \mathbf{w}_g, \mathbf{w}, \boldsymbol{\mu}_g) \quad (12a)$$

$$= \inf_{\mathbf{w}_g} \sup_{\mathbb{Q}_g \in \mathcal{A}_{\varepsilon_g, 1, d}^{(g)}(\Xi)} \mathbb{E}^{\mathbb{Q}_g}[\ell_H(\mathbf{w}_g; \boldsymbol{\xi})] + \frac{\rho}{2} \|\mathbf{w}_g - \mathbf{w} + \boldsymbol{\mu}_g\|_2^2 \quad (12b)$$

$$= \inf_{\mathbf{w}_g, \lambda_g \geq 0} \lambda_g \varepsilon_g + \frac{1}{N_g} \sum_{n_g=1}^{N_g} \sup_{\boldsymbol{\xi} \in \Xi} \left\{ \ell_H(\mathbf{w}_g; \boldsymbol{\xi}) - \lambda_g d(\boldsymbol{\xi}, \widehat{\boldsymbol{\xi}}_{n_g}) \right\} + \frac{\rho}{2} \|\mathbf{w}_g - \mathbf{w} + \boldsymbol{\mu}_g\|_2^2 \quad (12c)$$

$$= \begin{cases} \min_{\mathbf{w}_g, \lambda_g, s_{n_g}} & \lambda_g \varepsilon_g + \frac{1}{N_g} \sum_{n_g=1}^{N_g} s_{n_g} + \frac{\rho}{2} \|\mathbf{w}_g - \mathbf{w} + \boldsymbol{\mu}_g\|_2^2 \\ \text{s. t.} & \max\{0, 1 - \widehat{\mathbf{y}}_n \cdot \mathbf{w}_g^\top \widehat{\mathbf{x}}_n\} \leq s_{n_g} \quad \forall n \in [N_g], \\ & \max\{0, 1 + \widehat{\mathbf{y}}_n \cdot \mathbf{w}_g^\top \widehat{\mathbf{x}}_n\} - \kappa \lambda_g \leq s_{n_g} \quad \forall n \in [N_g] \\ & \lambda \geq \|\mathbf{w}_g\|_* \end{cases} \quad (12d)$$

where (12c) exploits the notable duality result presented in [9, 10] to rewrite the inner maximization problem as a minimization problem, and (12d) follows by introducing slack variables  $s_{n_g}$ , recalling that  $\ell(\boldsymbol{\xi})$  is convex, and utilizing similar arguments to the ones presented in the proof of Theorem 1 in [7]. Note that  $\|\cdot\|_*$  in the above is the dual to the norm used in the transportation cost function (3).

*Remark 4.* Note that the local client problem presented in (12d) is intended for the setting where  $\mathcal{X} = \mathbb{R}^P$ . This suggests that while still usable in settings where  $\mathcal{X} \subset \mathbb{R}^P$ , it may lead to a suboptimal model. Therefore, in settings where  $\mathcal{X}$  is bounded, we may instead utilize the SVM model from Corollary 3.12 in [15] for the local client problems.

Once all the clients solve for their optimal local models, they communicate them to the central server. The central server then obtains the optimal global model parameters  $\mathbf{w}^*$  by simply solving the following minimization problem

$$\mathbf{w}^* = \arg \min_{\mathbf{w}} \sum_{g=1}^G \alpha_g \frac{\rho}{2} \|\mathbf{w} - (\mathbf{w}_g + \boldsymbol{\mu}_g)\|_2^2. \quad (13)$$

We observe that the objective function in (13) is strongly convex, indicating that it has a unique minimizer  $\mathbf{w}^*$ , which can be obtained by setting its partial derivative with respect to  $\mathbf{w}$  to 0,

$$\sum_{g=1}^G \alpha_g \frac{\rho}{2} [2\mathbf{w}^* - 2(\mathbf{w}_g + \boldsymbol{\mu}_g)] = 0 \quad (14a)$$

$$\Leftrightarrow \sum_{g=1}^G \alpha_g \mathbf{w}^* = \sum_{g=1}^G \alpha_g (\mathbf{w}_g + \boldsymbol{\mu}_g) \quad (14b)$$

$$\Leftrightarrow \mathbf{w}^* = \sum_{g=1}^G \alpha_g (\mathbf{w}_g + \boldsymbol{\mu}_g), \quad (14c)$$

where (14c) follows by recalling that  $\sum_{g=1}^G \alpha_g = 1$ . Once the central server computes  $\mathbf{w}^*$ , it then sends it back to the clients, where the process repeats. Leveraging the previous results, we can write the ADMM algorithm explicitly as follows.

---

**Algorithm 2** ADMM Algorithm

---

**Input:**  $\mathbf{w}^{(0)}, \mathbf{w}_g^{(0)}, \boldsymbol{\mu}_g^{(0)}$ **Parameters:** Number of iterations  $T$ , scale parameter  $\rho$ **Output:**  $\mathbf{w}^*$ 

```
1: for  $t = 1, \dots, T$  do
2:   for clients  $g = 1, \dots, G$  do
3:      $\mathbf{w}_g^{(t+1)} \leftarrow \mathbf{w}_g^*$  minimizer of  $J_g(\mathbf{w}^{(t)}, \boldsymbol{\mu}_g^{(t)})$  (problem (12d))
4:   end for
5:    $\mathbf{w}^{(t+1)} \leftarrow \sum_{g=1}^G \alpha_g (\mathbf{w}_g^{(t+1)} + \boldsymbol{\mu}_g^{(t)})$ 
6:   for clients  $g = 1, \dots, G$  do
7:      $\boldsymbol{\mu}_g^{(t+1)} \leftarrow \boldsymbol{\mu}_g^{(t)} + \mathbf{w}_g^{(t+1)} - \mathbf{w}^{(t+1)}$ 
8:   end for
9: end for
```

---

### 5.3 Theoretical Analysis of Algorithms

Next, we investigate the theoretical convergence of both algorithms and we obtain their theoretical worst-case time complexity.

#### 5.3.1 SM Algorithm

We first present two lemmas required to guarantee convergence of the SM algorithm. Next, we explicitly establish its convergence, and proceed to analyze its time complexity to converge to an optimal solution with tolerance  $\epsilon_1$ .

**Lemma 2** (SM Objective Function Convexity). *Suppose Assumption 4 holds and let  $f(\mathbf{w}) = \sum_{g=1}^G \alpha_g \sup_{\mathbb{Q}_g \in \mathcal{A}_{\epsilon_g, 1, d}^{(g)}(\Xi)} \mathbb{E}^{\mathbb{Q}_g} [\ell_H(\mathbf{w}; \boldsymbol{\xi})]$ . Then,  $f(\mathbf{w})$  is convex in  $\mathbf{w}$ .*

*Proof.* The proof is provided in the Appendix. □

**Lemma 3** (SM Objective Function Lipschitz Continuity). *Suppose Assumption 4 holds and let  $f(\mathbf{w}) = \sum_{g=1}^G \alpha_g \sup_{\mathbb{Q}_g \in \mathcal{A}_{\epsilon_g, 1, d}^{(g)}(\Xi)} \mathbb{E}^{\mathbb{Q}_g} [\ell_H(\mathbf{w}; \boldsymbol{\xi})]$ . Then,  $f(\mathbf{w})$  is Lipschitz continuous in  $\mathbf{w}$ .*

*Proof.* The proof is provided in the Appendix. □

**Theorem 1** (SM Algorithm Convergence). *The SM Algorithm 1 converges to an optimal solution  $\mathbf{w}^*$  of the problem in (5) with arbitrary tolerance  $\epsilon_1$  if the stepsize  $\gamma(t) \rightarrow 0$  as  $t \rightarrow \infty$  and  $\sum_{t=1}^{\infty} \gamma(t) = \infty$ .*

*Proof.* Note that it is established in [42] that the subgradient method is guaranteed convergence if three conditions hold: i) the objective function is convex, ii) the objective function is Lipschitz continuous, and iii) the step-size is diminishing an appropriate rate as stated in the Theorem statement. We verify the first two conditions in Lemmas 2 and 3, whereas the third condition can be ensured by choosing an appropriate step size. □

**Theorem 2** (SM Algorithm Time Complexity). *Suppose that the  $\ell_\infty$ -norm is used in the worst-case distribution problem (9), and that the barrier method equipped with the log barrier function and Newton updates is used to solve it. Then, the SM algorithm 1 equipped with an appropriately diminishing step-size [42] has a worst-case time complexity of  $\mathcal{O}(\epsilon_1^{-2} [N_{g^*}^{3.5} P^{3.5} \log(\epsilon_2^{-1}) + GP])$ , where  $\epsilon_1$  and  $\epsilon_2$  are the tolerances of the solutions of the subgradient method and the worst-case distribution problem (9), respectively, and  $N_{g^*}$  is the greatest number of samples available at any one client. This analysis can be directly extended to cases where other norms are used in (9).*

*Proof.* We begin by examining the time complexity of problem (9) that each client  $g$  solves at each iteration  $t$ . Note that when the  $\ell_\infty$ -norm is used in (9), the problem can be written as an LP with  $4N_g P + 2N_g$  decision variables (including slack variables) and  $4N_g P + 7N_g$  constraints, where  $N_g$  is the number of training samples at the  $g^{\text{th}}$  client. If this problem is solved via the barrier method equipped with the log barrier function and Newton updates, it would require  $\mathcal{O}(\sqrt{C} \log(\epsilon_2^{-1}))$  iterations to reach an  $\epsilon_2$ -solution [43], where  $C$  is the number of constraints. Moreover, each iteration would have an arithmetic complexity of  $\mathcal{O}(CD^2)$ , where  $D$  is the number of decision variables. Therefore, solving the problem in (9) via the previously stated method has a theoretical worst-case time complexity of

$$\mathcal{O}([4N_g P + 7N_g]^{1.5} [4N_g P + 2N_g]^2 \log(\epsilon_2^{-1})).$$

By eliminating scalar multipliers and constants, this result can be simplified to the following expression,

$$\mathcal{O}([N_g P]^{3.5} \log(\epsilon_2^{-1})).$$

Note that all clients can solve their local problems in parallel and will have the same number of features. Thus, the client with the largest number of samples  $N_{g^*}$  will have the highest time complexity. Furthermore, note that the central server performs a summation of  $G + 1$  vectors of dimension  $P$  during each iteration  $t$ , the time complexity of which is  $\mathcal{O}(GP)$ . We obtain the final result by noting that the subgradient method converges to a solution with tolerance  $\epsilon_1$  in  $\mathcal{O}(\epsilon_1^{-1})$  iterations [44]. Note that we do not explicitly consider the time complexity of computing the local subgradient at each client since it is lower than that of solving the problem in (9).  $\square$

### 5.3.2 ADMM Algorithm

Before we discuss the theoretical convergence of the ADMM algorithm, we first introduce the following lemma.

**Lemma 4** (ADMM Objective Properties). *Let  $f(\mathbf{w}_g) = \sup_{\mathbb{Q}_g \in \mathcal{A}_{\epsilon_g, 1, d}^{(g)}(\Xi)} \mathbb{E}^{\mathbb{Q}_g}[\ell_H(\mathbf{w}_g; \boldsymbol{\xi})]$ , then  $f(\mathbf{w}_g)$  is a closed proper convex function in  $\mathbf{w}_g$ .*

*Proof.* The proof is provided in the Appendix.  $\square$

Even though the client objective functions are closed proper convex functions as we demonstrate in Lemma 4, and strong duality holds as shown in [9, 10, 17], global convergence of the multi-block (i.e.  $G \geq 3$ ) ADMM algorithm in 2 is not guaranteed [45]. A counterexample is presented in [45] demonstrating that the multi-block ADMM with a separable convex objective function can fail to converge. However, the convergence of multi-block ADMM in many practical cases [46, 47] has motivated works to investigate conditions under which it is guaranteed convergence [48, 49]. In the following, we present conditions that guarantee convergence of the ADMM algorithm based on the results from [49].

**Theorem 3** (ADMM Algorithm Convergence). *The ADMM algorithm 2 converges to an optimal solution  $\mathbf{w}^*$  of the problem in (5) with arbitrary tolerance  $\epsilon_1$  if the local client problem (12d) is modified by adding a  $\tau_g \|\mathbf{w}_g\|_2^2$  term to each client's objective function where  $\tau_g$  are user-defined parameters, and  $\rho \leq$*

$$\min_{g=1, \dots, G-1} \left\{ \frac{4\alpha_g \tau_g}{g(2G+1-g)}, \frac{4\alpha_G \tau_G}{(G-1)(G+2)} \right\}.$$

*Proof.* The authors in [49] establish the convergence of multi-block ADMM in the setting where the objective functions of  $(B - 1)$  of the  $B$  blocks are strongly convex with strong convexity parameter  $\sigma_b$  for each block  $b$ . They formulate the problem to be solved via ADMM as follows:

$$\begin{aligned} \min \quad & f_1(\mathbf{v}_1) + f_2(\mathbf{v}_2) + \dots + f_B(\mathbf{v}_B) \\ \text{s. t.} \quad & \mathbf{A}_1 \mathbf{v}_1 + \mathbf{A}_2 \mathbf{v}_2 + \dots + \mathbf{A}_B \mathbf{v}_B = \mathbf{c} \\ & \mathbf{v}_b \in \mathcal{V}_b \quad \forall b \in [B], \end{aligned} \tag{15}$$

where  $f_b(\mathbf{v}_b)$  is the objective function term and  $\mathbf{v}_b$  is the decision variable associated with the  $b^{\text{th}}$  block.

Note that if we were to rewrite our problem from (11) in a similar form, there would be no distinction between the clients and the central server, and the objective function term associated with the central server would remain 0. Thus, we add a strongly convex term  $\tau_g \|\mathbf{w}_g\|_2^2$  to the objective function term associated with each of the clients to meet the requirement that  $B - 1$  of the blocks must have a strongly convex objective function. In the summation, each  $\tau_g \|\mathbf{w}_g\|_2^2$  term will be multiplied by its respective weight  $\alpha_g$ . Therefore, the strong convexity parameter associated with client  $g$  would be  $2\alpha_g \tau_g$ .

To rewrite problem (11) in the form of problem (15), the  $\mathbf{A}$  matrix associated with client  $g$  would be a block matrix of  $P \times P$  matrices stacked vertically in  $G$  blocks. The  $g^{\text{th}}$  block from the top would be the identity matrix, whereas all the other blocks would be zero. Similarly, the matrix associated with the central server would be a block matrix of similar structure but where all the blocks are the negative of the identity matrix. Incorporating this insight into the condition on  $\rho$  described in Theorem 3.3 in [49] allows us to obtain the final result.  $\square$

*Remark 5.* While this additional  $\tau_g \|\mathbf{w}_g\|_2^2$  term makes the objective functions strongly convex thereby theoretically guaranteeing convergence, it is also a redundant regularization term. This may negatively impact the accuracy of the final, which we study empirically in Section 6.

**Theorem 4** (Strongly Convex ADMM Algorithm Time Complexity). *Suppose that the  $\ell_1$ -norm is used in the strongly convex variant of the local model problem (12d), and that the barrier method equipped with the log barrier function and Newton updates is used to solve it. Then, the ADMM algorithm 2 equipped with  $\rho$  chosen according to Theorem 3 has a worst-case time complexity of  $\mathcal{O}(\epsilon_1^{-1} [(N_{g^*} + P)^{3.5} \log(\epsilon_2^{-1}) + GP])$ , where  $\epsilon_1$  and  $\epsilon_2$  are the tolerances of the solutions of ADMM and the strongly convex variant of the local model problem (12d), respectively, and  $N_{g^*}$  is the largest number of samples at any one client.*

*Proof.* We begin by studying the complexity of solving the strongly convex variant of the local model problem in (12d) solved by each client during each iteration  $t$ . Using the  $\ell_1$ -norm, we can express our problem as a QCQP with  $N_g + 2P + 3$  decision variables (including slack variables) and  $2N_g + 2P + 3$  constraints. This can be solved using the barrier method equipped with the log barrier function and Newton updates. For this class of problems, the aforementioned method requires  $\mathcal{O}(\sqrt{C} \log(\epsilon_2^{-1}))$  iterations to reach an  $\epsilon_2$ -solution, where  $C$  is the number of constraints [43]. Each iteration has an arithmetic complexity of  $\mathcal{O}([C + D]D^2)$ , where  $D$  is the number of decision variables [43]. Therefore, solving the problem via the previously discussed method has a complexity of

$$\mathcal{O}([2N_g + 2P + 3]^{0.5} [3N_g + 4P + 6][N_g + 2P + 3]^2 \log(\epsilon_2^{-1})).$$

By eliminating scalar multipliers and constants, the problem can be simplified to the following:

$$\mathcal{O}([N_g + P]^{3.5} \log(\epsilon_2^{-1})).$$

Similar to the previous algorithm, all clients can solve their local problems in parallel and will have the same number of features. Thus the client with the greatest number of samples  $N_{g^*}$  will have the problem with the greatest time complexity. Furthermore, we note that the central server aggregates  $2G$  vectors of dimension  $P$  in each iteration, the time complexity of which is  $\mathcal{O}(GP)$ . Therefore, we obtain the final result by noting that ADMM converges to an  $\epsilon_1$ -solution in  $\mathcal{O}(\epsilon_1^{-1})$  iterations assuming the strong convexity of the objective function and that the upper bound on  $\rho$  is satisfied [49]. While each client  $g$  also performs the update of the local scaled Lagrange multipliers  $\mu_g$  during each iteration, this process has a much lower complexity than solving the local problem and is, therefore, not explicitly considered in this analysis.  $\square$

*Remark 6.* In our time complexity analysis, we only considered the setting where the  $\ell_\infty$ -norm is utilized in the transportation cost function 3. This analysis can be directly extended to settings where  $\ell_1$  or  $\ell_2$ -norm are used.

## 5.4 A Brief Note on Communication Costs

Observe that in the SM algorithm, each client sends a vector of length  $P$  to the central server during each iteration, and receives a vector of length  $P$  in return. Since  $G$  clients participate in this training process over  $T$  iterations, the total number of numerical values shared in this process is  $2PGT$ . Similarly, the total number of numerical values shared in the ADMM algorithm is  $3PGT$ . However, in a centralized scheme, the clients would need to share all their data of total size  $PN$  with the central server, and would receive model parameters of size  $P$  once the server has completed training. This highlights that our proposed problem and its associated SM and ADMM algorithms are only advantageous from a shared data volume reduction perspective when  $(N + 1)P \gg 2PGT$  and  $(N + 1)P \gg 3PGT$ , respectively. Our proposed problem setting and algorithms are also massively advantageous in settings where preserving data privacy is desired.

## 6 Numerical Experiments

In all the experiments presented in this section we utilize identical weights  $\alpha_g$  for all clients  $g \in [G]$ , regardless of the number of clients or training samples available at each client. This is used as a naïve baseline to examine the performance of our proposed model and algorithms. Moreover, note that all the error bars presented on the plots or confidence intervals presented numerically correspond to a single standard deviation. The datasets we use in our experiments are the following:

- i. *Triplex Reciprocating Pump Fault Classification Dataset [50]*: This is a simulation dataset that uses a Simulink model to simulate the healthy and faulty operation of a reciprocating pump. This dataset is used in the Sensitivity Analysis Experiment. The generated simulation data belongs to two classes: healthy pump and leak fault. We focus on the binary classification problem since binary classification models can directly extend to multiclass problems via a one-vs-all framework as mentioned previously. Therefore, performance in the binary setting is indicative of that in the multiclass setting. However, data is generated to simulate different severities of the leak fault, where each client has a different severity to simulate data heterogeneity across clients. Features extracted from the time series data (such as kurtosis and skewness) are used for classification.

- ii. *make\_classification Simulation Dataset* [51]: The simulation data generated using this module belongs to two classes, each of which contains data sampled from a standard Gaussian distribution with means located at vertices of a  $P$ -dimensional hypercube with sides of length 2.4 centered at the origin. This data is used in the Scalability Experiment due to the flexibility in the number of features and number of samples of the generated data.
- iii. *UCI Repository Datasets*: We utilize seven datasets from the UCI repository to validate our proposed model and compare it with baselines in the Real-World Experiment. Namely, the datasets we use are Banknote [52], Breast Cancer Wisconsin (BCW) [53], Connectionist Bench (CB) [54], Mammographic Mass [55], Parkinson’s [56], Rice [57], and User Knowledge Modeling (UKM) [58]. Note that in the UKM dataset the ‘Very Low’ and ‘Low’ classes are lumped into one class, whereas the ‘Middle’ and ‘High’ classes are lumped into another.

In the numerical experiments we evaluate the performance of the following models and algorithms:

- i. *Central*: This is an implementation of the centralized DR-SVM with hinge loss and with the assumption of unbounded feature support, introduced in [15]. This model serves as a benchmark where all the data can be moved to a central location and model training can be done in a centralized fashion.
- ii. *SM*: This is our proposed FDR-SVM model in (5) solved via the SM algorithm in 1. In our implementation of this algorithm we use a stepsize  $\gamma(t)$  at iteration  $t$  that diminishes according to  $\gamma(t) = \gamma/t$ , where  $\gamma$  is the initial stepsize, and is treated as a model parameter.
- iii. *ADMM*: This is our proposed FDR-SVM model in (5) solved via the ADMM algorithm in 2. While this algorithm is not theoretically guaranteed convergence, we show empirically that in all our experiments it can converge to a model with competitive performance.
- iv. *ADMM-SC*: This is our proposed FDR-SVM model in (5) with an additional strongly convex regularization term as discussed in 3, solved via the ADMM algorithm in 2. In our implementation we set the regularization parameter  $\tau_g$  equivalently for all clients  $g \in [G]$  as the minimum value it can take calculated from the condition in Theorem 3 to minimize the magnitude of redundant regularization.
- v. *ADMM-REG*: This is a regularized version of our proposed model, solved via the ADMM algorithm in 2. However, we set  $\kappa = \infty$  to obtain this regularized version of our model, which is explained in [7]. This model serves as another benchmark where distributional robustness is not implemented into the model, but the model is still trained in a distributed fashion.

## 6.1 Experiment 1: Sensitivity Analysis

In this experiment we examine the performance of our proposed model and its solution algorithms measured via mean correct classification rate (mCCR) as their parameters change. We separate the model and algorithm parameters into 2 groups: global, and local. The global parameters pertain to the solution algorithms, as they are the total number of iterations  $T$ , and the initial stepsize  $\gamma$  or scale parameter  $\rho$  for the SM and ADMM algorithms, respectively. The local parameters pertain to the DR-SVM, as they are the local label flipping cost  $\kappa_g$ , and the local Wasserstein ball radius factor  $\beta_g$ , where the ball radius is  $\varepsilon_g = \frac{1}{\beta_g} N_g$ . Note that while the local parameters can be set differently for each client, for the sake of simplicity we only study settings where they are equivalent for all clients. In this experiment set we study 5 distinct settings: i) nominal, where training data is distributed evenly across clients and classes, ii) client imbalance, where the training data distribution across clients is [70%, 15%, 10%, 5%] iii) class imbalance, where the training data distribution across classes is [90%, 10%], iv) client + class imbalance, which is a combination of the previous two settings, and v) noisy labels, where 15% of the labels of training samples are flipped. While setting (i) examines model performance in a perfectly balanced setting, this is highly unlikely in a real-world setting. In fact, in an industrial fault classification setting client imbalance will arise from each of the customers collecting different volumes of data from their equipment, whereas class imbalance will arise from the abundance of healthy operation data and shortage of fault data. This is because faults are usually repaired soon after they occur. Finally, the noisy labels setting emulates the data mislabeling that can result from human error.

In all the settings studied we use  $G = 4$ ,  $P = 14$ ,  $N = 400$ , and  $N_{Test} = 1000$  test samples. The test set contains 500 healthy samples, and 125 samples from each of the 4 fault severities. Furthermore, for the ADMM-SC algorithm we utilize  $\tau_g = 18\rho$ , which is the minimum value  $\tau_g$  can take while maintaining guaranteed convergence according to the condition in Theorem 3. Each experiment is repeated 50 times, with the data being randomly shuffled during each repetition. We evaluate the mCCR of all the models tested across the 50 repetitions. For all the studies presented in this experiment we evaluate the performance of the central model for  $\varepsilon \in \{1 \times 10^b\}_{b=-5}^{-1}$  and  $\kappa \in \{0.1, 0.25, 0.5, 0.75, 1\}$ , and we only report the peak performance achieved. We provide further detail on each of the global and local experiments next.

### 6.1.1 Global Parameters

In the global parameter experiment we evaluate the performance of both the SM and ADMM algorithms for  $T \in \{5, 10, 20, 60, 100, 140, 180, 220\}$  and  $\rho, \gamma \in \{1 \times 10^b\}_{b=-3}^3$ . We fix  $\varepsilon_g = \frac{1}{10N_g}$  and  $\kappa_g = 0.5$  for each client  $g$ . While such values of  $\varepsilon_g$  and  $\kappa_g$  may not be optimal, we use them to demonstrate that our proposed model can perform well when compared to the baselines. Any further improvement of parameter choices via cross-validation (CV) can only improve the model performance. The results of this experiment are reported in Figure 1.

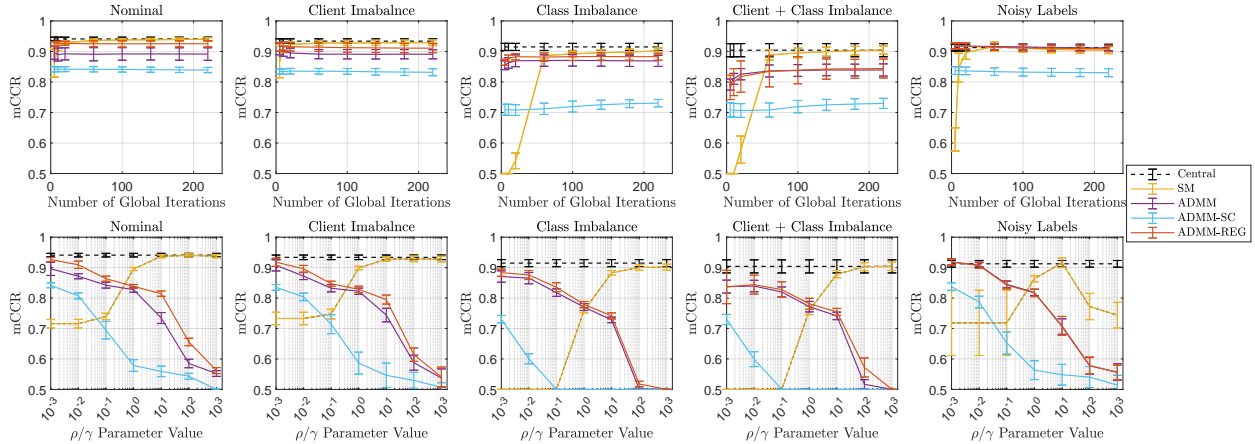


Figure 1: Plots of mCCR vs. the global parameters for both the SM and ADMM algorithms compared with the best performing centralized DR SVM (Central), the strongly convex ADMM algorithm (ADMM-SC), and the regularized federated SVM (ADMM-REG).

We make multiple observations from the experimental results. Firstly, we observe that the SM algorithm outperforms all the other distributed models, and achieves very similar performance to the central model. Moreover, it is less sensitive to changes in  $\gamma$  than the ADMM algorithms are to changes in  $\rho$  as it maintains its peak performance for a wider range of the parameter. This performance, however, comes at the cost of training time, as it requires more iterations than the ADMM algorithms to reach its peak performance in many cases. Moreover, the performance of the SM algorithm seems to be much less affected by client and class imbalance and their combination than ADMM algorithms, making it a good choice in settings where such imbalance is known to exist. Secondly, we make the surprising observation that the FDR-SVM trained via the ADMM algorithm is outperformed by its regularized counterpart (ADMM-REG) in all but the noisy labels setting. However, this can be explained by noting that the key difference between the two models is that the DR model accounts for label uncertainty via the label flipping cost parameter  $\kappa$ , unlike the regularized model [7]. This can make the FDR-SVM equipped with a relatively low  $\kappa$  too conservative where all the training labels are correct. Indeed, this is further confirmed when we note that the FDR-SVM slightly outperforms its regularized counterpart in the noisy label setting. We note, however, that with appropriate local parameter choices ADMM can still outperform ADMM-REG as we show in the local parameter experiment. Additionally, we observe that ADMM-SC is consistently outperformed by ADMM and ADMM-REG, which can be expected due to the redundant regularization provided by the additional strongly convex term. Indeed, observe that the performance of ADMM-SC drops more significantly than that of ADMM and ADMM-REG as  $\rho$  increases. This is because increasing  $\rho$  leads to increasing  $\tau$ , which increases the magnitude of redundant regularization and impacts model performance. Finally, and also very surprisingly, we observe that ADMM and ADMM-REG very slightly outperform the centralized model in the noisy label setting. This is unexpected as the centralized model typically outperform distributed ones. This may indicate that the central model is highly sensitive to its parameters in this setting. Alternatively, we could explain this result by noting that our proposed FDR-SVM uses a *different ambiguity set* from the central model's. This may suggest that our proposed MoWB ambiguity set is more successful at modeling uncertainty than the traditional Wasserstein ball in certain settings.

### 6.1.2 Local Parameters

In this experiment we evaluate the performance of both the SM and ADMM algorithms for  $\varepsilon_g = \frac{1}{\beta N_g}$  where  $\beta \in \{0.1, 1, 10, 100\}$  and for  $\kappa_g = \kappa \in \{0.1, 0.25, 0.5, 0.75, 1\}$ . We fix  $T = 220$  and  $\gamma = 1 \times 10^2$  and  $T = 100$  and  $\gamma = 1 \times 10^{-3}$  for the SM and ADMM algorithms, respectively. The results of this experiment are reported in Figure 2.

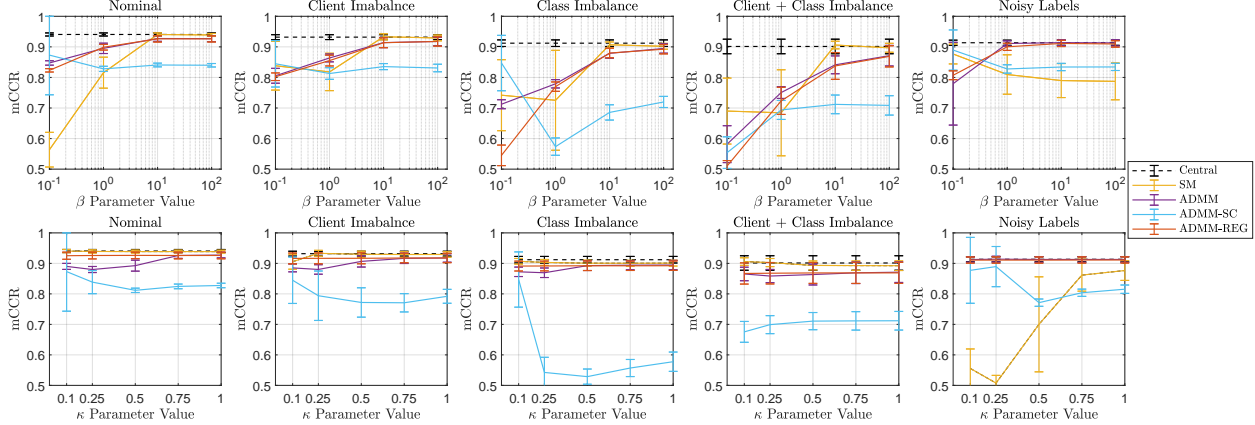


Figure 2: Plots of mCCR vs. the local parameters for both the SM and ADMM algorithms compared with the best performing centralized DR SVM (Central), the strongly convex ADMM algorithm (ADMM-SC), and the regularized federated SVM (ADMM-REG).

A key observation that can be made from the results is that with low  $\kappa$  values, ADMM is outperformed by ADMM-REG. However, ADMM matches, and in some cases, exceeds the performance of ADMM-REG as  $\kappa$  increases. This confirms our hypothesis that ADMM was outperformed by ADMM-REG in the global parameter experiment due to the over-conservatism of the DR model equipped with low  $\kappa$  values. This result indeed confirms that the FDR-SVM will always perform just as well as its regularized counterpart, if not better, in many settings including uncertain training labels. We also observe that SM is less sensitive than ADMM to the choice of  $\kappa$  for all settings except for the noisy label setting, exhibiting almost opposite behavior to ADMM. Moreover, SM is also relatively highly sensitive to the choice of local Wasserstein radius. Indeed, in most settings the performance of SM improves as the local radius decreases. However, for noisy labels performance drops as the local radius decreases. This is likely due to the need for larger local ambiguity sets to account for both feature and label uncertainty. Additionally, we observe again that SM’s peak performance is higher than that of ADMM in all settings except for noisy labels. This is because the results of the global parameter experiment show that SM achieves peak performance in this setting with  $\gamma = 1 \times 10^1$ . However, in this experiment we test with  $\gamma = 1 \times 10^2$ . Thus, by referencing the previous experiment’s results we see that SM would still perform just as well as ADMM given appropriately chosen parameters. Another observation we make is that ADMM-SC is once again outperformed by all the other models for most parameter values due to redundant regularization. A surprising result, however, is that in some settings the error bars of the ADMM-SC exceed all the other models in performance, even the central model. This again suggests that the MoWB ambiguity set may be able to characterize the uncertainty better than the traditional Wasserstein ball in some settings.

## 6.2 Experiment 2: Scalability Experiment

This experiment examines the scalability of the algorithms and models under study using simulation data generated via the `make_classification` module [51]. The data distribution across clients and across classes is identical to that utilized in the nominal setting of the previous experiment. We test the following settings: a) *Increasing clients [fixed training samples]*:  $N = 1000$ ,  $P = 4$ ,  $G \in \{10, 20, 30, 40, 50\}$ ; b) *Increasing clients [increasing training samples]*:  $N = 100G$ ,  $P = 4$ ,  $G \in \{10, 20, 30, 40, 50\}$ ; c) *Increasing training samples*:  $G = 10$ ,  $P = 4$ ,  $N \in \{1000, 1500, 2000, 2500, 3000\}$ , and d) *Increasing features*:  $N = 4$ ,  $G = 10$ ,  $P \in \{4, 6, 8, 10, 12\}$ . It is important to note that the subgradient method lacks a practically implementable stopping criterion [59], while no stopping criterion is provided for multi-block ADMM in [49]. Thus, we opt for evaluating scalability in the same fashion for all algorithms: we compute the mean runtime in seconds over 50 repetitions required by each algorithm to converge to the model with the highest mCCR. During each repetition, we use new randomly generated training and test sets. For the SM algorithm we test performance for  $T \in \{140, 180, 220\}$  and  $\gamma \in \{1 \times 10^b\}_{b=1}^3$ . Meanwhile, for the ADMM algorithms we test performance for  $T \in \{10, 20, 30\}$  and  $\gamma \in \{1 \times 10^b\}_{b=-3}^{-1}$ . For all algorithms, we fix  $\varepsilon_g = \frac{1}{10N_g}$  and  $\kappa = 0.25$ . The central model we trained is tuned in an identical fashion to that from the previous experiment, and the reported runtime is that taken to solve the optimization problem. The results of this study are reported in Figure 3.

The results in Figure 3 reflect a rough trend of increasing runtime as  $N$  and  $P$  increase for all models due to the increasing complexity of the local client problems. However, the trend is clearer with the SM algorithm, whereas it is noisy with all versions of the ADMM algorithm, and is hardly observable with the central model. This could be

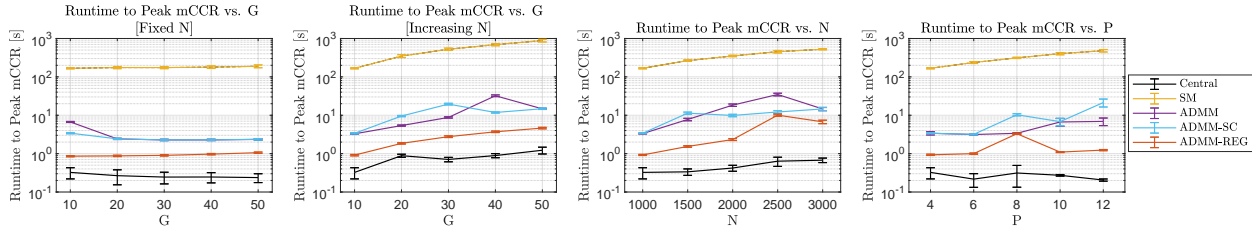


Figure 3: Plots of time to reach peak mCCR vs. the number of clients  $G$  with fixed and increasing  $N$ , the number of features  $P$ , and the number of training samples  $N$  for all models tested.

attributed to the fact that the SM algorithm requires a much longer time to reach peak mCCR, making the effect of random computer system variations minimal on the reported time. On the contrary, all versions of the ADMM and the central model reach peak mCCR in a very short time, making the reported time highly susceptible to system variations. These results highlight the fact that any performance gains achieved by using SM come at the cost of a much longer runtime. However, the runtime of ADMM and ADMM-SC is comparable to that of ADMM-REG. Additionally, we observe that the runtime remains roughly constant for all three models as  $G$  increases if  $N$  is fixed. This is because a fixed  $N$  makes the local problem at each client increasingly simpler and faster to solve as  $G$  increases. In contrast, when both  $G$  and  $N$  are increasing we observe that all algorithms exhibit a trend of increasing runtime with the number of clients.

### 6.3 Experiment 3: Real-World Experiments

This experiment utilizes real-world datasets from the UCI repository to examine the performance of our proposed model and algorithms in various realistic settings. We perform 50 repetitions of each experiment, where the data is randomly shuffled during each repetition. We utilize 70% of the data as a training set, and the remaining 30% as a test set for all datasets. We fix  $G = 4$ ,  $\kappa_g = 1$  and  $\varepsilon_g = \frac{1}{10N_g}$ , and we test with  $T \in \{5, 10, 20, 60, 100, 140, 180, 220\}$  and  $\rho, \gamma \in \{1 \times 10^b\}_{b=-3}^3$  for all distributed models. For the centralized model, we test with  $\varepsilon \in \{1 \times 10^b\}_{b=-5}^{-1}$  and  $\kappa \in \{0.1, 0.25, 0.5, 0.75, 1\}$ . We utilize the F-1 score to assess model performance due to possible class imbalance, and we report results in Table 1.

Table 1: Peak F-1 score attained by classification models on 7 real-world datasets

Dataset	Central	SM	ADMM	ADMM-SC	ADMM-REG
Banknote	<b>0.951</b> $\pm$ 0.012	0.855 $\pm$ 0.018	<b>0.951</b> $\pm$ 0.012	0.949 $\pm$ 0.012	<b>0.951</b> $\pm$ 0.012
BCW	0.968 $\pm$ 0.011	0.957 $\pm$ 0.014	<b>0.970</b> $\pm$ 0.011	0.957 $\pm$ 0.012	0.964 $\pm$ 0.010
CB	0.760 $\pm$ 0.044	0.779 $\pm$ 0.052	<b>0.784</b> $\pm$ 0.049	0.767 $\pm$ 0.046	<b>0.784</b> $\pm$ 0.051
Mammographic Mass	0.798 $\pm$ 0.020	0.796 $\pm$ 0.019	<b>0.800</b> $\pm$ 0.020	0.799 $\pm$ 0.020	<b>0.800</b> $\pm$ 0.020
Parkinson’s	0.921 $\pm$ 0.028	<b>0.925</b> $\pm$ 0.015	0.914 $\pm$ 0.017	0.906 $\pm$ 0.019	0.912 $\pm$ 0.016
Rice	<b>0.939</b> $\pm$ 0.005	0.936 $\pm$ 0.006	<b>0.939</b> $\pm$ 0.005	0.938 $\pm$ 0.005	0.938 $\pm$ 0.004
UKM	0.850 $\pm$ 0.024	<b>0.851</b> $\pm$ 0.024	<b>0.851</b> $\pm$ 0.022	0.799 $\pm$ 0.020	0.850 $\pm$ 0.022

The results of this experiment reveal that one or more of our proposed algorithms for our FDR-SVM attain the highest F-1 score for all datasets. However, we observe that ADMM outperforms SM on most datasets, which was not the case in Experiment 1. In fact, the only dataset where SM outperforms ADMM is Parkinson’s, which is a dataset with high class imbalance ([75%, 25%]). This suggests that the performance of the FDR-SVM in terms of F-1 score depends largely on the choice of algorithm. Therefore, in a real-world setting the choice of algorithm should be made based on factors such as guaranteed theoretical convergence, runtime until convergence, and the results of initial preliminary experiments on the dataset under study. We also observe that the performance of ADMM-SC can be significantly lower than that of ADMM on datasets such as BCW and UKM, but it also can be almost identical to it on datasets such as Banknote, Mammographic Mass, and Rice. This highlights that guaranteed theoretical convergence *need not always come at a significant sacrifice in model performance*, further emphasizing the need for preliminary experimentation when one of those algorithms is being chosen for a real-world problem. Another observation we make is that ADMM-REG attains the same performance as ADMM on some datasets, whereas it falls short of it on most. As demonstrated in Experiment 1, this is most likely due to label uncertainty levels. More specifically, ADMM-REG will perform very similarly to ADMM on datasets where the labels have some uncertainty, whereas it will be outperformed on datasets with noisy labels. Finally, a very surprising observation is that the centralized model does not attain the peak F-1 score

on most datasets. This again suggests that our proposed MoWB ambiguity set may lead to performance improvements over the traditional Wasserstein ball in some settings.

## 7 Conclusions

In this work we proposed a novel FDR-SVM model, which is trained in a distributed manner by  $G$  clients and a central server, and can be used in distributed fault diagnosis tasks without data sharing. To achieve this, we proposed a novel MoWB ambiguity set that allows for the natural separability of the FDR-SVM problem. Subsequently, we demonstrated that the ambiguity set inherits out-of-sample performance guarantees from the local Wasserstein balls under certain assumptions. We then proposed two distinct algorithms that can be used to train the FDR-SVM: a subgradient method-based algorithm and an ADMM-based one. We studied the convergence of both algorithms, demonstrating conditions required for theoretical convergence and deriving their time complexities. Finally, we evaluated the performance of our proposed model through a series of simulation and real-world experiments, demonstrating that it outperforms existing benchmarks in many settings of practical interest.

## References

- [1] S. Bollapragada, A. Gupta, and C. Lawsirirat, “Managing a portfolio of long term service agreements,” *EUROPEAN JOURNAL OF OPERATIONAL RESEARCH*, vol. 182, pp. 1399–1411, NOV 1 2007.
- [2] M. Seera and C. P. Lim, “Online motor fault detection and diagnosis using a hybrid fmm-cart model,” *IEEE TRANSACTIONS ON NEURAL NETWORKS AND LEARNING SYSTEMS*, vol. 25, pp. 806–812, APR 2014.
- [3] Y. Li, Z. Zhou, C. Sun, X. Chen, and R. Yan, “Variational attention-based interpretable transformer network for rotary machine fault diagnosis,” *IEEE TRANSACTIONS ON NEURAL NETWORKS AND LEARNING SYSTEMS*, 2022 SEP 12 2022.
- [4] N. Dutta, P. Kaliannan, and P. Shanmugam, “Svm algorithm for vibration fault diagnosis in centrifugal pump,” *INTELLIGENT AUTOMATION AND SOFT COMPUTING*, vol. 35, no. 3, pp. 2997–3020, 2023.
- [5] B. McMahan, E. Moore, D. Ramage, S. Hampson, and B. A. y. Arcas, “Communication-Efficient Learning of Deep Networks from Decentralized Data,” in *Proceedings of the 20th International Conference on Artificial Intelligence and Statistics* (A. Singh and J. Zhu, eds.), vol. 54 of *Proceedings of Machine Learning Research*, pp. 1273–1282, PMLR, 20–22 Apr 2017.
- [6] J. Du, N. Qin, D. Huang, Y. Zhang, and X. Jia, “An efficient federated learning framework for machinery fault diagnosis with improved model aggregation and local model training,” *IEEE TRANSACTIONS ON NEURAL NETWORKS AND LEARNING SYSTEMS*, vol. 35, pp. 10086–10097, JUL 2024.
- [7] S. Shafieezadeh Abadeh, P. M. Mohajerin Esfahani, and D. Kuhn, “Distributionally robust logistic regression,” in *Advances in Neural Information Processing Systems* (C. Cortes, N. Lawrence, D. Lee, M. Sugiyama, and R. Garnett, eds.), vol. 28, Curran Associates, Inc., 2015.
- [8] A. J. Kleywegt, A. Shapiro, and T. Homem-de Mello, “The sample average approximation method for stochastic discrete optimization,” *SIAM Journal on Optimization*, vol. 12, no. 2, pp. 479–502, 2002.
- [9] D. Kuhn, P. M. Esfahani, V. A. Nguyen, and S. Shafieezadeh-Abadeh, *Wasserstein Distributionally Robust Optimization: Theory and Applications in Machine Learning*, ch. 6, pp. 130–166. INFORMS, 2019.
- [10] P. Mohajerin Esfahani and D. Kuhn, “Data-driven distributionally robust optimization using the wasserstein metric: performance guarantees and tractable reformulations,” *Mathematical Programming*, vol. 171, pp. 115–166, 2018.
- [11] H. E. Scarf, K. Arrow, and S. Karlin, *A min-max solution of an inventory problem*. Rand Corporation Santa Monica, 1957.
- [12] E. Delage and Y. Ye, “Distributionally robust optimization under moment uncertainty with application to data-driven problems,” *Operations Research*, vol. 58, no. 3, pp. 595–612, 2010.
- [13] G. Bayraksan and D. Love, *Data-Driven Stochastic Programming Using Phi-Divergences*, pp. 1–19. INFORMS, 10 2015.
- [14] A. Shapiro, “Distributionally robust stochastic programming,” *SIAM Journal on Optimization*, vol. 27, no. 4, pp. 2258–2275, 2017.
- [15] S. Shafieezadeh-Abadeh, D. Kuhn, and P. M. Esfahani, “Regularization via mass transportation,” 2019.

- [16] A. Ben-Tal, D. den Hertog, A. De Waegenaere, B. Melenberg, and G. Rennen, “Robust solutions of optimization problems affected by uncertain probabilities,” *Management Science*, vol. 59, no. 2, pp. 341–357, 2013.
- [17] R. Gao and A. Kleywegt, “Distributionally robust stochastic optimization with wasserstein distance,” *Mathematics of Operations Research*, vol. 48, no. 2, pp. 603–655, 2023.
- [18] A. Cherukuri and J. Cortés, “Cooperative data-driven distributionally robust optimization,” *IEEE Transactions on Automatic Control*, vol. 65, no. 10, pp. 4400–4407, 2020.
- [19] F. Lin, S.-C. Fang, X. Fang, and Z. Gao, “Distributionally robust chance-constrained kernel-based support vector machine,” *Computers & Operations Research*, vol. 170, p. 106755, 2024.
- [20] S. Sagawa, P. W. Koh, T. B. Hashimoto, and P. Liang, “Distributionally robust neural networks for group shifts: On the importance of regularization for worst-case generalization,” 2020.
- [21] X. Zhou and X. Wang, “A memory-efficient federated kernel support vector machine for edge devices,” *IEEE Transactions on Neural Networks and Learning Systems*, pp. 1–13, 2023.
- [22] H. Yang, S. Liang, J. Ni, H. Li, and X. S. Shen, “Secure and efficient k nn classification for industrial internet of things,” *IEEE Internet of Things Journal*, vol. 7, no. 11, pp. 10945–10954, 2020.
- [23] A. Selvi, M. R. Belbasi, M. B. Haugh, and W. Wiesemann, “Wasserstein logistic regression with mixed features,” in *Advances in Neural Information Processing Systems* (A. H. Oh, A. Agarwal, D. Belgrave, and K. Cho, eds.), 2022.
- [24] D. Faccini, F. Maggioni, and F. A. Potra, “Robust and distributionally robust optimization models for linear support vector machine,” *Computers & Operations Research*, vol. 147, p. 105930, 2022.
- [25] T. Wu, R. Zheng, T. Gui, Q. Zhang, and X. Huang, “Modeling the q-diversity in a min-max play game for robust optimization,” 2023.
- [26] F. Sattler, S. Wiedemann, K.-R. Mueller, and W. Samek, “Robust and communication-efficient federated learning from non-i.i.d. data,” *IEEE TRANSACTIONS ON NEURAL NETWORKS AND LEARNING SYSTEMS*, vol. 31, pp. 3400–3413, SEPT 2020.
- [27] J. Xu, W. Du, Y. Jin, W. He, and R. Cheng, “Ternary compression for communication-efficient federated learning,” *IEEE TRANSACTIONS ON NEURAL NETWORKS AND LEARNING SYSTEMS*, vol. 33, pp. 1162–1176, MAR 2022.
- [28] A. Z. Tan, H. Yu, L. Cui, and Q. Yang, “Towards personalized federated learning,” *IEEE Transactions on Neural Networks and Learning Systems*, vol. 34, no. 12, pp. 9587–9603, 2023.
- [29] F. Sattler, K.-R. Müller, and W. Samek, “Clustered federated learning: Model-agnostic distributed multitask optimization under privacy constraints,” *IEEE Transactions on Neural Networks and Learning Systems*, vol. 32, no. 8, pp. 3710–3722, 2021.
- [30] X. Zhou and X. Wang, “Memory and communication efficient federated kernel k-means,” *IEEE Transactions on Neural Networks and Learning Systems*, vol. 35, no. 5, pp. 7114–7125, 2024.
- [31] A. Ponomarenko-Timofeev, O. Galinina, R. Balakrishnan, N. Himayat, S. Andreev, and Y. Koucheryavy, “Multi-task model personalization for federated supervised svm in heterogeneous networks,” 2023.
- [32] H. Wang, M. Xiao, C. Wu, and J. Zhang, “Distributed classification for imbalanced big data in distributed environments,” *Wireless Networks*, pp. 1–12, 2021.
- [33] Y. Lu, V. Roychowdhury, and L. Vandenberghe, “Distributed parallel support vector machines in strongly connected networks,” *IEEE Transactions on Neural Networks*, vol. 19, no. 7, pp. 1167–1178, 2008.
- [34] Y. Deng, M. M. Kamani, and M. Mahdavi, “Distributionally robust federated averaging,” in *Advances in Neural Information Processing Systems* (H. Larochelle, M. Ranzato, R. Hadsell, M. Balcan, and H. Lin, eds.), vol. 33, pp. 15111–15122, Curran Associates, Inc., 2020.
- [35] C. Wu and H. Wang, “A fast distributed accelerated gradient algorithm for big data classification,” in *2022 IEEE Intl Conf on Dependable, Autonomic and Secure Computing, Intl Conf on Pervasive Intelligence and Computing, Intl Conf on Cloud and Big Data Computing, Intl Conf on Cyber Science and Technology Congress (DASC/PiCom/CBDCCom/CyberSciTech)*, pp. 1–8, 2022.
- [36] M. Zecchin, M. Kountouris, and D. Gesbert, “Communication-efficient distributionally robust decentralized learning,” 2023.
- [37] T. T.-K. Lau and H. Liu, “Wasserstein distributionally robust optimization with wasserstein barycenters,” 2022.
- [38] D. Bertsimas and M. Sim, “The price of robustness,” *Operations Research*, vol. 52, no. 1, pp. 35–53, 2004.

- [39] L. Kantorovitch, “On the translocation of masses,” *Doklady Akademii Nauk USSR*, vol. 37, pp. 227–229, 1942.
- [40] J. Mathew, C. K. Pang, M. Luo, and W. H. Leong, “Classification of imbalanced data by oversampling in kernel space of support vector machines,” *IEEE TRANSACTIONS ON NEURAL NETWORKS AND LEARNING SYSTEMS*, vol. 29, pp. 4065–4076, SEP 2018.
- [41] J.-B. Hiriart-Urruty and C. Lemaréchal, *Convex Analysis and Minimization Algorithms I*. Springer, 1 ed., 1993.
- [42] Y. Nesterov, *Introductory lectures on convex optimization: A basic course*, vol. 87. Springer Science & Business Media, 2013.
- [43] Y. Nesterov and A. Nemirovskii, *Interior-Point Polynomial Algorithms in Convex Programming*. Society for Industrial and Applied Mathematics, 1994.
- [44] S. Bubeck, “Convex optimization: Algorithms and complexity,” *Foundations and Trends® in Machine Learning*, vol. 8, no. 3-4, pp. 231–357, 2015.
- [45] C. Chen, B. He, Y. Ye, and X. Yuan, “The direct extension of admm for multi-block convex minimization problems is not necessarily convergent,” *Mathematical Programming*, vol. 155, no. 1, pp. 57–79, 2016.
- [46] Y. Peng, A. Ganesh, J. Wright, W. Xu, and Y. Ma, “Rasl: Robust alignment by sparse and low-rank decomposition for linearly correlated images,” *IEEE transactions on pattern analysis and machine intelligence*, vol. 34, no. 11, pp. 2233–2246, 2012.
- [47] M. Tao and X. Yuan, “Recovering low-rank and sparse components of matrices from incomplete and noisy observations,” *SIAM Journal on Optimization*, vol. 21, no. 1, pp. 57–81, 2011.
- [48] W. Deng, M.-J. Lai, Z. Peng, and W. Yin, “Parallel multi-block admm with  $o(1/k)$  convergence,” *Journal of Scientific Computing*, vol. 71, pp. 712–736, 2017.
- [49] T.-Y. Lin, S.-Q. Ma, and S.-Z. Zhang, “On the sublinear convergence rate of multi-block admm,” *Journal of the Operations Research Society of China*, vol. 3, pp. 251–274, 2015.
- [50] Mathworks, “Multi-class fault detection using simulated data.”
- [51] F. Pedregosa, G. Varoquaux, A. Gramfort, V. Michel, B. Thirion, O. Grisel, M. Blondel, P. Prettenhofer, R. Weiss, V. Dubourg, J. Vanderplas, A. Passos, D. Cournapeau, M. Brucher, M. Perrot, and E. Duchesnay, “Scikit-learn: Machine learning in Python,” *Journal of Machine Learning Research*, vol. 12, pp. 2825–2830, 2011.
- [52] V. Lohweg, “Banknote Authentication.” UCI Machine Learning Repository, 2013. DOI: <https://doi.org/10.24432/C55P57>.
- [53] W. Wolberg, O. Mangasarian, N. Street, and W. Street, “Breast Cancer Wisconsin (Diagnostic).” UCI Machine Learning Repository, 1995. DOI: <https://doi.org/10.24432/C5DW2B>.
- [54] T. Sejnowski and R. Gorman, “Connectionist Bench (Sonar, Mines vs. Rocks).” UCI Machine Learning Repository. DOI: <https://doi.org/10.24432/C5T01Q>.
- [55] M. Elter, “Mammographic Mass.” UCI Machine Learning Repository, 2007. DOI: <https://doi.org/10.24432/C53K6Z>.
- [56] M. Little, “Parkinsons.” UCI Machine Learning Repository, 2008. DOI: <https://doi.org/10.24432/C59C74>.
- [57] I. Cınar and M. Koklu, “Rice (Cammeo and Osmanlık).” UCI Machine Learning Repository, 2019. DOI: <https://doi.org/10.24432/C5MW4Z>.
- [58] H. Kahraman, I. Colak, and S. Sagiroglu, “User Knowledge Modeling.” UCI Machine Learning Repository, 2013. DOI: <https://doi.org/10.24432/C5231X>.
- [59] A. Bagirov, N. Karimtsa, and M. M. Mäkelä, *Subgradient Methods*, pp. 295–297. Cham: Springer International Publishing, 2014.
- [60] S. Boyd and L. Vandenberghe, *Convex optimization*. Cambridge university press, 2004.
- [61] C. D. Aliprantis and K. C. Border, *Convexity*, pp. 251–305. Heidelberg: Springer-Verlag Berlin, 2006.
- [62] D. Bertsekas, *Convex Optimization Theory*. Athena Scientific optimization and computation series, Athena Scientific, 2009.

## Appendix

**Lemma 5.** Any two real scalars  $a, a' \in \mathbb{R}$  obey the following

$$|\max\{0, a\} - \max\{0, a'\}| \leq |a - a'|.$$

*Proof.* To see this, consider the following cases:

1.  $a, a' \geq 0$ . In this case one can directly see that

$$|\max\{0, a\} - \max\{0, a'\}| = |a - a'|$$

2.  $a \geq 0, a' < 0$ . In this case, we have the following:

$$\begin{aligned} |\max\{0, a\} - \max\{0, a'\}| &= a < |a| + |a'| \\ &= |a - a'|. \end{aligned}$$

3.  $a < 0, a' \geq 0$ . This is symmetric to the previous case.

4.  $a < 0, a' < 0$ . In this case we have the following:

$$|\max\{0, a\} - \max\{0, a'\}| = 0 \leq |a - a'|.$$

□

### Proof of Lemma 2

*Proof.* Since  $\ell_H(\mathbf{w}, \boldsymbol{\xi})$  is a maximum of linear terms in  $\mathbf{w}$ , then it is convex in  $\mathbf{w}$ . Moreover, sums, scalar multiplication, taking the supremum, and the expectation are all operations that preserve convexity [60]. Thus,  $f(\mathbf{w})$  is convex in  $\mathbf{w}$ . □

### Proof of Lemma 3

*Proof.* As discussed in [15], if assumption 4 holds then one can obtain the discrete distribution described in (8) that attains the worst case risk. Therefore, we have the following:

$$\begin{aligned} f(\mathbf{w}) &= \sum_{g=1}^G \alpha_g f_g(\mathbf{w}) \\ &:= \sum_{g=1}^G \alpha_g \left( \frac{1}{N_g} \sum_{n_g=1}^{N_g} \beta_{n_g}^{+*} \ell_H(\mathbf{w}; (\hat{y}_{n_g}, \hat{\mathbf{z}}_{n_g}^+)) + \beta_{n_g}^{-*} \ell_H(\mathbf{w}; (-\hat{y}_{n_g}, \hat{\mathbf{z}}_{n_g}^-)) \right), \end{aligned}$$

Now, suppose we have  $\mathbf{w}$  and  $\mathbf{w}'$  which correspond to worst-case distributions characterized by  $(\beta_{n_g}^{\pm*}, \hat{\mathbf{z}}_{N_g}^{\pm})$  and  $(\beta_{n_g}^{\pm' *}, \hat{\mathbf{z}}_{N_g}^{\pm'})$ , respectively. Then we can write the following:

$$\begin{aligned} &|f_g(\mathbf{w}) - f_g(\mathbf{w}')| \\ &= \frac{1}{N_g} \left| \sum_{n_g=1}^{N_g} \left[ \beta_{n_g}^{+*} \ell_H(\mathbf{w}; (\hat{y}_{n_g}, \hat{\mathbf{z}}_{n_g}^+)) + \beta_{n_g}^{-*} \ell_H(\mathbf{w}; (-\hat{y}_{n_g}, \hat{\mathbf{z}}_{n_g}^-)) \right] \right. \\ &\quad \left. - \sum_{n_g=1}^{N_g} \left[ \beta_{n_g}^{+'*} \ell_H(\mathbf{w}'; (\hat{y}_{n_g}, \hat{\mathbf{z}}_{n_g}^{+'})) + \beta_{n_g}^{-' *} \ell_H(\mathbf{w}'; (-\hat{y}_{n_g}, \hat{\mathbf{z}}_{n_g}^{-'})) \right] \right| \end{aligned} \tag{16a}$$

$$\begin{aligned} &\leq \frac{1}{N_g} \left| \sum_{n_g=1}^{N_g} \left[ \beta_{n_g}^{+*} \ell_H(\mathbf{w}; (\hat{y}_{n_g}, \hat{\mathbf{z}}_{n_g}^+)) - \beta_{n_g}^{+'*} \ell_H(\mathbf{w}'; (\hat{y}_{n_g}, \hat{\mathbf{z}}_{n_g}^{+'})) \right] \right| \\ &\quad + \left| \sum_{n_g=1}^{N_g} \left[ \beta_{n_g}^{-*} \ell_H(\mathbf{w}; (-\hat{y}_{n_g}, \hat{\mathbf{z}}_{n_g}^-)) - \beta_{n_g}^{-' *} \ell_H(\mathbf{w}'; (-\hat{y}_{n_g}, \hat{\mathbf{z}}_{n_g}^{-'})) \right] \right| \end{aligned} \tag{16b}$$

$$\begin{aligned} &\leq \frac{1}{N_g} \sum_{n_g=1}^{N_g} \left[ \left| \beta_{n_g}^{+*} \ell_H(\mathbf{w}; (\hat{y}_{n_g}, \hat{z}_{n_g}^+)) - \beta_{n_g}^{+I*} \ell_H(\mathbf{w}'; (\hat{y}_{n_g}, \hat{z}_{n_g}^{+I})) \right| \right. \\ &\quad \left. + \left| \beta_{n_g}^{-*} \ell_H(\mathbf{w}; (-\hat{y}_{n_g}, \hat{z}_{n_g}^-)) - \beta_{n_g}^{-I*} \ell_H(\mathbf{w}'; (-\hat{y}_{n_g}, \hat{z}_{n_g}^{-I})) \right| \right] \end{aligned} \quad (16c)$$

$$\begin{aligned} &\leq \frac{1}{N_g} \sum_{n_g=1}^{N_g} \left[ \left| \beta_{n_g}^{+*} \ell_H(\mathbf{w}; (\hat{y}_{n_g}, \hat{z}_{n_g}^+)) - \beta_{n_g}^{+*} \ell_H(\mathbf{w}'; (\hat{y}_{n_g}, \hat{z}_{n_g}^+)) \right| \right. \\ &\quad \left. + \left| \beta_{n_g}^{-*} \ell_H(\mathbf{w}; (-\hat{y}_{n_g}, \hat{z}_{n_g}^-)) - \beta_{n_g}^{-*} \ell_H(\mathbf{w}'; (-\hat{y}_{n_g}, \hat{z}_{n_g}^-)) \right| \right] \end{aligned} \quad (16d)$$

$$\begin{aligned} &\leq \frac{1}{N_g} \sum_{n_g=1}^{N_g} \left[ \left| \beta_{n_g}^{+*} \max\{0, 1 - \hat{y}_{n_g} \cdot \mathbf{w}^\top \hat{z}_{n_g}^+\} - \beta_{n_g}^{+*} \max\{0, 1 - \hat{y}_{n_g} \cdot \mathbf{w}'^\top \hat{z}_{n_g}^+\} \right| \right. \\ &\quad \left. + \left| \beta_{n_g}^{-*} \max\{0, 1 + \hat{y}_{n_g} \cdot \mathbf{w}^\top \hat{z}_{n_g}^-\} - \beta_{n_g}^{-*} \max\{0, 1 + \hat{y}_{n_g} \cdot \mathbf{w}'^\top \hat{z}_{n_g}^-\} \right| \right] \end{aligned} \quad (16e)$$

$$= \frac{1}{N_g} \sum_{n_g=1}^{N_g} \left[ \left| (\mathbf{w}' - \mathbf{w})^\top (\beta_{n_g}^{+*} \cdot \hat{y}_{n_g} \cdot \hat{z}_{n_g}^+) \right| + \left| (\mathbf{w} - \mathbf{w}')^\top (\beta_{n_g}^{-*} \cdot \hat{y}_{n_g} \cdot \hat{z}_{n_g}^-) \right| \right] \quad (16f)$$

$$\leq \frac{1}{N_g} \sum_{n_g=1}^{N_g} \|\mathbf{w} - \mathbf{w}'\| \left( \left\| \beta_{n_g}^{+*} \cdot \hat{y}_{n_g} \cdot \hat{z}_{n_g}^+ \right\|_* + \left\| \beta_{n_g}^{-*} \cdot \hat{y}_{n_g} \cdot \hat{z}_{n_g}^- \right\|_* \right) \quad (16g)$$

$$= \|\mathbf{w} - \mathbf{w}'\| \left[ \frac{1}{N_g} \sum_{n_g=1}^{N_g} \left\| \beta_{n_g}^{+*} \cdot \hat{y}_{n_g} \cdot \hat{z}_{n_g}^+ \right\|_* + \left\| \beta_{n_g}^{-*} \cdot \hat{y}_{n_g} \cdot \hat{z}_{n_g}^- \right\|_* \right], \quad (16h)$$

where (16b) and (16c) follow from the triangle inequality, and (16d) follows by noting that the distribution characterized by  $(\beta_{n_g}^{\pm I*}, \hat{z}_{n_g}^{\pm I})$  maximizes the expected risk with respect to  $\mathbf{w}'$ , thus the distribution characterized by  $(\beta_{n_g}^{\pm*}, \hat{z}_{n_g}^{\pm})$  will at most attain the same risk with respect to  $\mathbf{w}'$ . Additionally, (16e) follows from the definition of the hinge loss function, (16f) follows from Lemma 5, and (16g) follows from the Cauchy-Schwarz inequality, where  $\|\cdot\|_*$  is the dual norm of  $\|\cdot\|$  used to measure distances in the space of  $\mathbf{w}$ . Given the previous, we can obtain the final result as follows:

$$|f(\mathbf{w}) - f(\mathbf{w}')| = \left| \sum_{g=1}^G \alpha_g f_g(\mathbf{w}) - \sum_{g=1}^G \alpha_g f_g(\mathbf{w}') \right| \quad (17a)$$

$$\leq \sum_{g=1}^G \alpha_g |f_g(\mathbf{w}) - f_g(\mathbf{w}')| \quad (17b)$$

$$\leq \|\mathbf{w} - \mathbf{w}'\| \sum_{g=1}^G \alpha_g \text{Lip}(f_g(\mathbf{w})), \quad (17c)$$

where (17b) follows from the triangle inequality and  $\text{Lip}(f_g(\mathbf{w}))$  is taken from (16h).  $\square$

#### Proof of Lemma 4

*Proof.* Recall that  $\ell_H(\mathbf{w}_g, \boldsymbol{\xi})$  is convex in  $\mathbf{w}_g$ , and taking the supremum and expectation are operations that preserve convexity [60], thus  $f(\mathbf{w}_g)$  is convex in  $\mathbf{w}_g$ . Now, note that

$$\ell_H(\mathbf{w}_g, \boldsymbol{\xi}) \geq 0 \Rightarrow f(\mathbf{w}_g) \geq 0 \quad \forall \mathbf{w}_g \in \mathbb{R}^P.$$

Now, observe that  $f(\mathbf{0}) = 0$  since  $\ell_H(\mathbf{0}, \boldsymbol{\xi}) = 0 \quad \forall \boldsymbol{\xi} \in \Xi$ . Since  $f(\mathbf{w}_g) > -\infty$  and it has a nonempty effective domain, then it is proper convex [61]. Finally, since  $f(\mathbf{w}_g) : \mathbb{R}^P \rightarrow (-\infty, \infty]$  is proper convex, then it is continuous by Proposition 1.3.11 in [62]. This implies the closedness of the function.  $\square$